Maximizing Performance from Loudspeaker Ports*

ALEX SALVATTI,[1] *AES Member*, **ALLAN DEVANTIER,[2]** *AES Member*, **AND DOUG J. BUTTON,[1]** *AES Member*

[1]*JBL Professional, Northridge, CA 91329, USA*

[2]*Infinity Systems, Northridge, CA 91329, USA*

There is a current trend in the marketplace for loudspeaker ports to have a more aerodynamic appearance. While this may be as much for appearance as for performance reasons, the sharp discontinuity at the end of a traditional port does create turbulence which negatively affects most performance parameters. Ports altered to provide a more aerodynamic shape to minimize turbulence for both the inlet and the exit air streams show performance improvements in efficiency, acoustic compression, maximum output, and distortion reduction. The ideal port shapes for high-velocity inlet and exit air streams are different, and the best solution is one that balances both. In addition turbulence is actually preferred in matters of cooling the box through heat exchange via the air in the port.

0 INTRODUCTION

Loudspeaker ports are generally used to augment the low-frequency acoustic output by supplying a Helmholtz resonator. At resonance, the inertance of the vent resonates with the compliance of the air in the cabinet, and the system acts as an acoustic impedance transformer presenting a high impedance to the rear of the loudspeaker cone and a low impedance to the air [1]. This increases the acoustic output over a limited low-frequency range compared to a sealed-box design. Several complications occur in vented designs as the output is increased beyond the point where the air in the port is able to respond in a linear fashion. They include undesirable extraneous noises generated within the port as well as acoustic compression and distortion. These generally broad-band "chuffing" noises due to fast moving air have been dealt with (since the late 1970s; see [2]) by rounding the port ends with various radii, which led to the now common flared port.

Recent studies by Vanderkooy [3], [4], Backman [5], and Roozen et al. [6] suggest that performance advantages can be achieved by providing a more aerodynamic profile throughout the length of the port. In addition, it is important that this aerodynamic profile be on both the entrance and the exit of the port.

Due to a longer "end correction," as discussed in Section 3.3, the tapered port also behaves as if it were longer than a straight ducted port. This is very useful for use in compact systems, where the port length is often restricted. Our investigational method for measuring port performance utilizes a microphone for pressure measurements and a hot-wire anemometer for velocity. Extensive benchmarking of current designs reveals that current attempts at high-output ports suffer from compression effects at high drive, showing that at very high levels all ports eventually "lock up," limiting the maximum output. At very high drive levels the air in the port becomes turbulent. Measurements show the velocity and pressure moving from a reactive relationship to a resistive one at high levels. At these levels the output from the port is 180° out of phase with the output of the cone, creating a nearly complete cancellation of low-frequency energy.

This paper includes a preliminary discussion on the history of loudspeaker port performance in Section 1 and on theoretical issues in Section 2. Section 3 presents 10 studies as follows:

- Section 3.1 examines acoustic port compression in straight versus radiused ports, showing that the former compresses to a much greater degree.
- Section 3.2 expands on the preceding by developing the utility of the Reynolds number as a general description of flow dynamics.
- Section 3.3 introduces a novel method to model a generalized flared port and presents an empirical formula to predict the tuning of a flared port accurately.
- Section 3.4 explores port compression among various flare rates, showing that there is a tradeoff between greater output at low levels and output at high levels.
- Section 3.5 examines how port profiles affect distortion,

* Presented at the 105th Convention of the Audio Engineering Society, San Francisco, CA, 1998 September 26–29; revised 2001 October 16.

finding that once again there exists a tradeoff between performance at low SPL and at high SPL. We discuss the effect of port profile on odd-order distortion and the implications of port symmetry on even harmonic distortion.
- Section 3.6 discusses velocity profile measurements made across different ports and how the results point to one profile as a preferred condition.
- Section 3.7 tests the hypothesis that port wall roughness imparts some performance improvements, finding that in fact roughness is detrimental to distortion and compression.
- Section 3.8 presents the same type of data as Sections 3.4 and 3.5 using a different mathematical port profile, but shows that the same conclusions and tradeoffs apply.
- Section 3.9 expands on the importance of port symmetry for lowest even-order distortion.
- Section 3.10 concludes the work by discussing the thermal implications of port design and placement, introducing the concept of port turbulence as a benefit to cooling.

Some general conclusions about designing ports of maximum performance are presented in Section 4.

1 HISTORY

As early as 1980 (Laupman [2]) patents started to surface, suggesting that flaring the end of ports was beneficial (Fig. 1). There exist also many good studies on turbulent effects in pipes dating back much further. In 1968 Ingard and Ising [7] studied the nature of compression and distortion in orifices. Fig. 2 [7] shows the effects of compression on the SPL with increasing level, and Fig. 3 illustrates the nonlinear behavior of high SPL and the resulting harmonic content from a symmetrical orifice driven at high level. Note that the odd harmonics are much stronger, a point we will discuss in Section 3.5. Fig. 4 also shows how at very high velocities the quadrature (reactive) relationship between velocity and pressure in the orifice disappears and the two are nearly in phase at high levels. This is particularly interesting because if the port pressure is in phase with velocity, the output of the port (which is now in phase with the back side of the cone) will be 180° out of phase with the front of the cone. In this condition the output in the far field could be reduced significantly in a bass reflex loudspeaker.

Extensive studies by Young [8] in 1975 and by Harwood [1] in 1972 outline expected performance limitations of traditional straight ports. Young points to a maximum velocity of about 10 m/s before serious sonic detriment occurs to the signal. In Fig. 5 Harwood shows the maximum allowable SPL for various pipe diameters

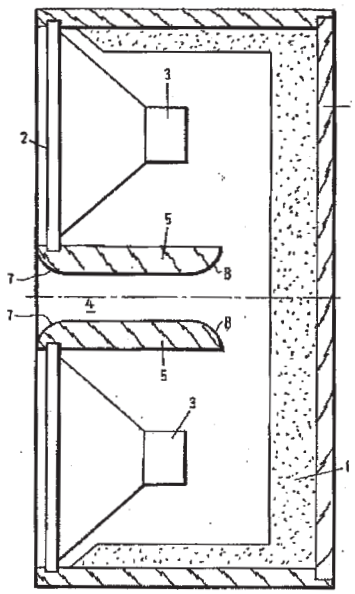

Fig. 1. Early loudspeaker design with radii on both ends of a port. (From Laupman [2].)

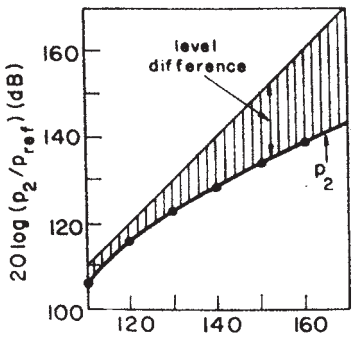

Fig. 2. SPL transmitted through an orifice in a plate as a function of driving sound pressure p_1. Shaded portion shows difference in level (compression) of p_1 and p_2. (From Ingard and Ising [7].)

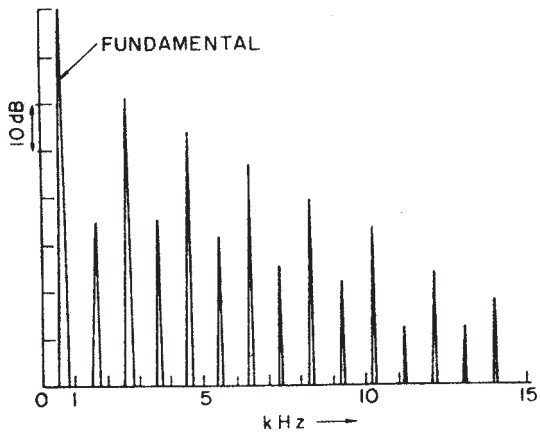

Fig. 3. Harmonic content of a pressure wave transmitted through an orifice in a plate of 162-dB driving SPL. Note dominance of odd-order harmonics. (From Ingard and Ising [7].)

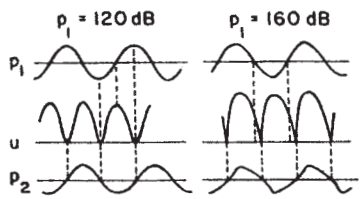

Fig. 4. Traces of pressure p and velocity u at low and high SPL in an orifice. At low SPL p_1 and p_2 are in quadrature; at high SPL they are in phase. p_1 represents pressure from backside of cone; p_2 is radiated sound from port. (From Ingard and Ising [7].)

before appreciable distortion due to turbulence ensues. Both authors point to a need for ports to be large in order that they produce greater SPL before losses and distortion become intolerable, the bottom line being to limit the velocity to below about 10 m/s. Both allude to turbulence being generated as the Reynolds number becomes too high, this being the cause of performance degradation. The degradation takes the form of broad-band noise, harmonic distortion, and compression.

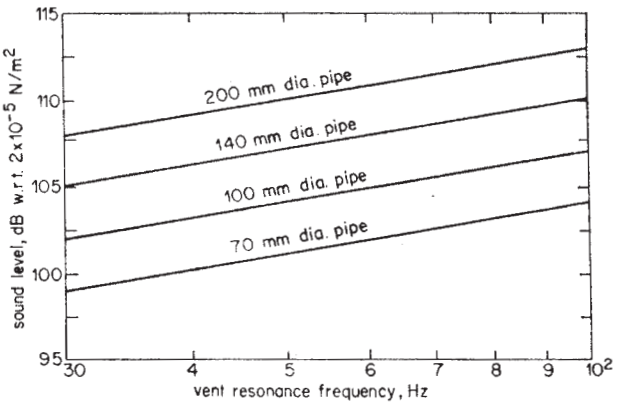

Fig. 5. Minimum SPL in a room of 2000 ft^3 (56.6 m^3) for various-diameter long pipes and vent resonant frequencies before distortion is appreciable. Note that the larger the pipe, the better, and doubling the area improves performance by 10 dB. Also lower tuning requires a larger pipe. (From Harwood [1].)

More recently, in 1995, Backman [5] showed the effects of adding very small radii to the ends of ports. The study shows a reduction in the distortion when adding even such a small change. Fig. 6 shows the difference in distortion and compression measured by Backman after radiusing the ends of the ports. Recent patents by Roozen et al. [6] showed a rather slow taper as being optimum. Roozen et al. display some very informative finite element analysis plots in Figs. 7 and 8, showing the vortex shedding as the air exits on a highly radiused port and on a slow taper port. The more flared port shows the vortices being generated inside the port, whereas the straighter port shows the vortex shedding occurring nearer the port ends. Also, the magnitude of the vortices is less in the slow taper port.[1]

[1] For more information on vortex shedding see [6].

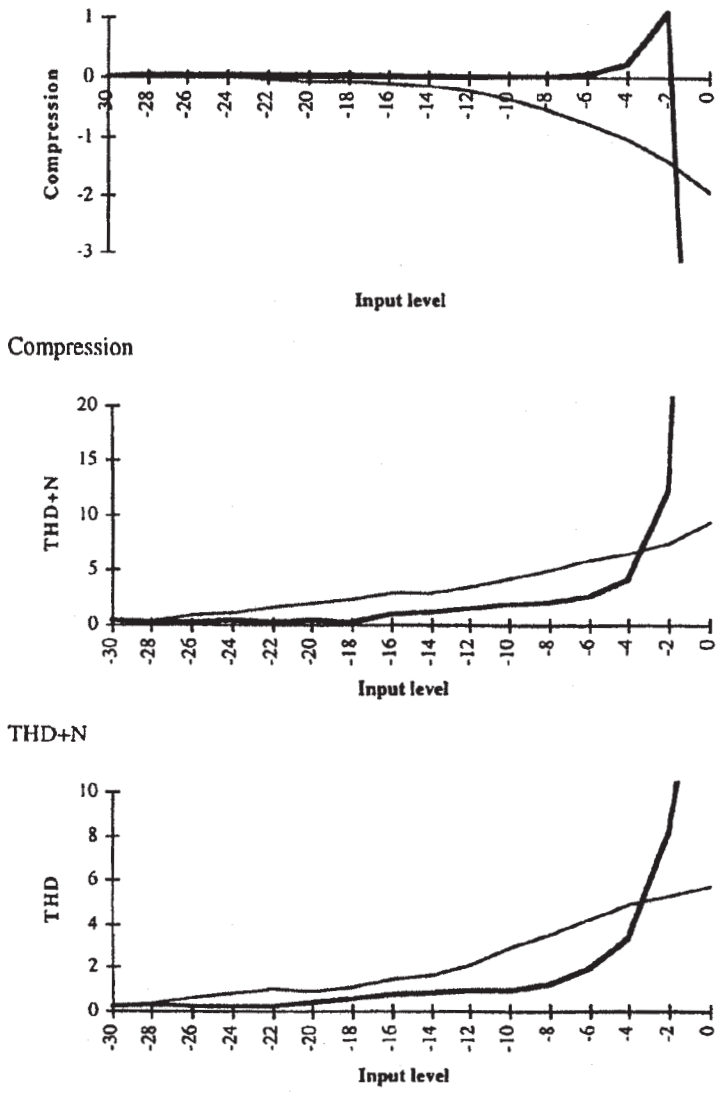

Fig. 6. Changes in distortion and compression. Lighter trace—straight port; heavier trace—port with small radii at both ends. (From Backman [5].)

This study shows that for high exit velocities a slower taper may be required, but it neglects to take into account that as an inlet a more extreme flare might actually be preferred. Granowski and Caron's 1998 patent [9] (Fig. 9) claims that an ellipsoidal flare is preferred. A further invention, outlined in patents by Polk and Campbell [10] (Fig. 10) and Goto [11] (Fig. 11), describes radiused ports with a plunger on the exit that smoothly directs the port velocity 90º in all directions to the outer periphery of the port. The previous study by Backman [5] showed that forcing the air to make any kind of turn will cause turbulence to occur at lower levels and is to be avoided if possible. However, these designs may have the great benefit of making the port effectively longer and useful in redirecting the airflow, which otherwise might exist straight into a wall or floor.

Figs. 12 and 13 are from a patent by Gahm [12]. The basic invention is a modular kit for making port tubes with radiused ends. Fig. 13 is particularly interesting as it shows a method for using the port velocity to cool the loudspeaker driver directly.

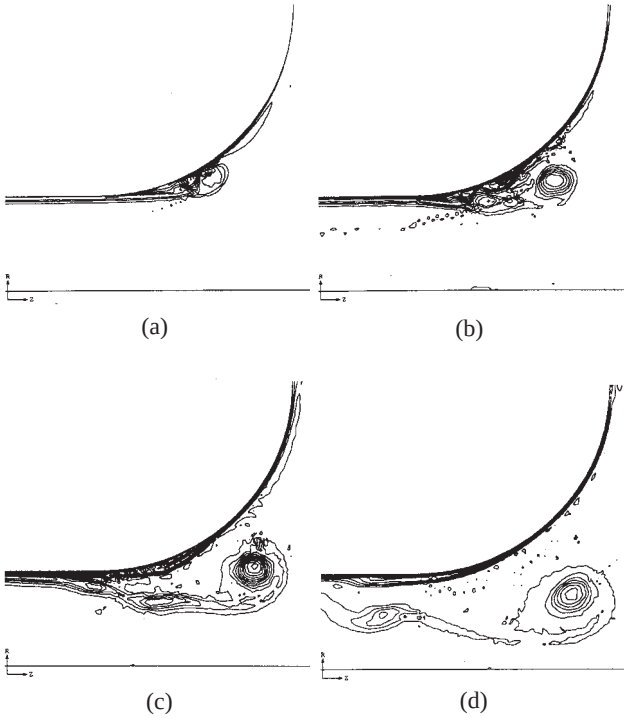

Fig. 7. Simulation of vortex shedding in highly radiused port on exit stroke. Note how early in the throat shedding begins. (From Roozen et al. [6].) (a) t = 7 ms. (b) t = 9 ms. (c) t = 11 ms. (d) t = 13 ms.

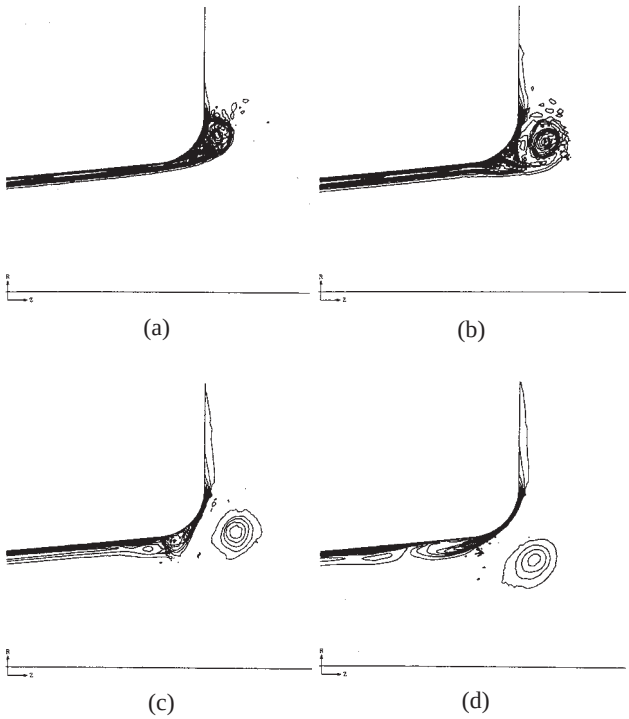

Fig. 8. Simulation of vortex shedding from very slow taper port. (From Roozen et al. [6].) (a) t = 7 ms. (b) t = 9 ms. (c) t = 11 ms. (d) t = 13 ms.

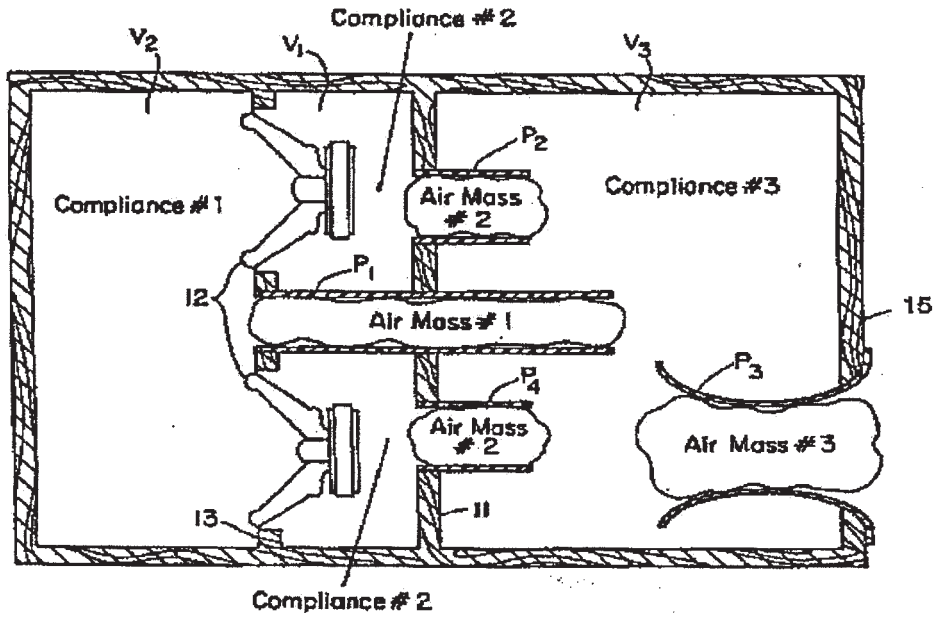

Fig. 9. Port 3 is shown with an elliptical cross section, which is said to be optimum. (From Gawronski and Caron [9].)

The most extensive and recent work on the topic comes from Vanderkooy [3], [4], [13]. This work is showing detailed measurements of port velocities and pressure waveforms, presents waveform analysis, and outlines a detailed methodology for taking the data. In Figs. 14 and 15 we see the waveform distortions at progressively higher levels o a straight and a radiused port. Note that the straight port develops a rather asymmetrical waveform with high levels of both odd and even harmonics. The radiused (at both ends) port, however, generates a more symmetrical wave, resembling a square wave with largely odd harmonics only. In Fig. 16 Vanderkooy reports on compression effects on several ports with a variety of interesting mathematical descriptions. While no one profile stands out as superior, an interesting observation of the data (also shown by Backman) shows that at medium to higher levels, a small amount of gain takes place before compression sets in. This might suggest that boundary-layer separation is beginning but is very small and provides a more aerodynamic flow of the air in the center of the port, which is still laminar. Vanderkooy was also able to develop a model and present the supporting measurements that show that at high SPL the in-box pressure and the port throat velocity are in phase, supporting Ingard. This clearly supports the earlier contention that at high levels the output from the port will be out of phase with the front of the driver in a bass reflex enclosure and will add additional compression, possibly completely canceling the fundamental. *The port is now simply a leak in the box*. As the cone moves inward, air exits the port in the opposite direction, and the resulting volume of displaced air is reduced. Vanderkooy shows detailed measurements and analyses of the exit jet formation at high levels, which support much of the analysis of Roozen et al. It is also important to examine closely the dynamics of the air during the inlet stroke.

2 FLUID-FLOW THEORY

Fluid flow is a very complex field, and rigorous solutions to some problems, such as the fine-scale random fluctuations in turbulent flow, defy closed-form solutions. In fact, there are no analyses, not even computer solutions, that exist to describe turbulent flow completely. Luckily there are some simplifications that can be made for the flow in loudspeaker ports. The most important is the assumption of incompressible flow, that is, density fluctuations are negligible. This simplifies the general continuity equation:

$$\frac{\partial \rho}{\partial t} + \nabla \cdot \rho \tilde{v} = 0 \tag{1}$$

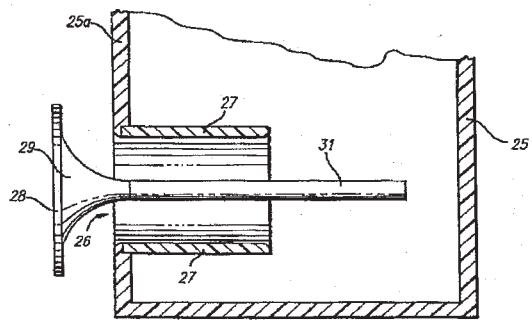

Fig. 10. Center fixture is said to improve aerodynamics and reduce air noise. (From Polk and Campbell [10].)

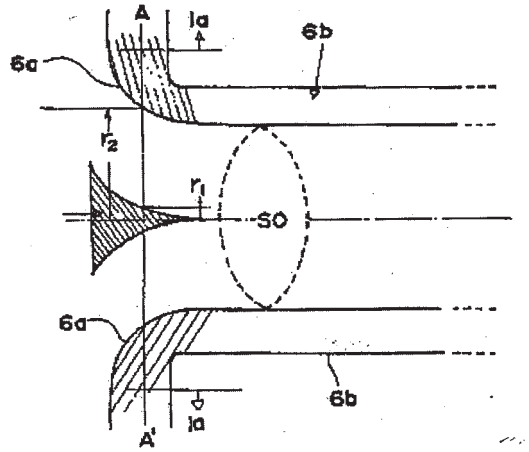

Fig. 11. Similar but earlier version of the Polk idea. (From Goto [11].)

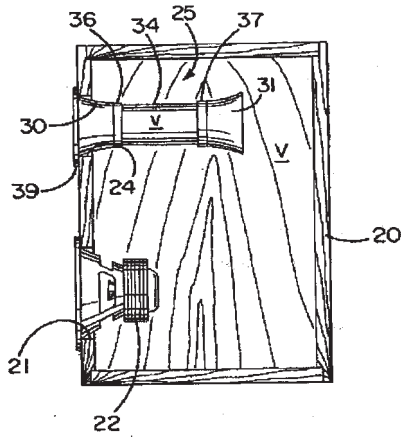

Fig. 12. Modular design for adding radii to a straight port. (From Gahm [12].)

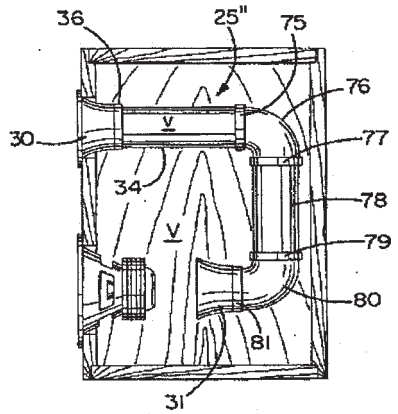

Fig. 13. Further refinement of modular port concept which uses port for cooling transducer. (From Gahm [12].)

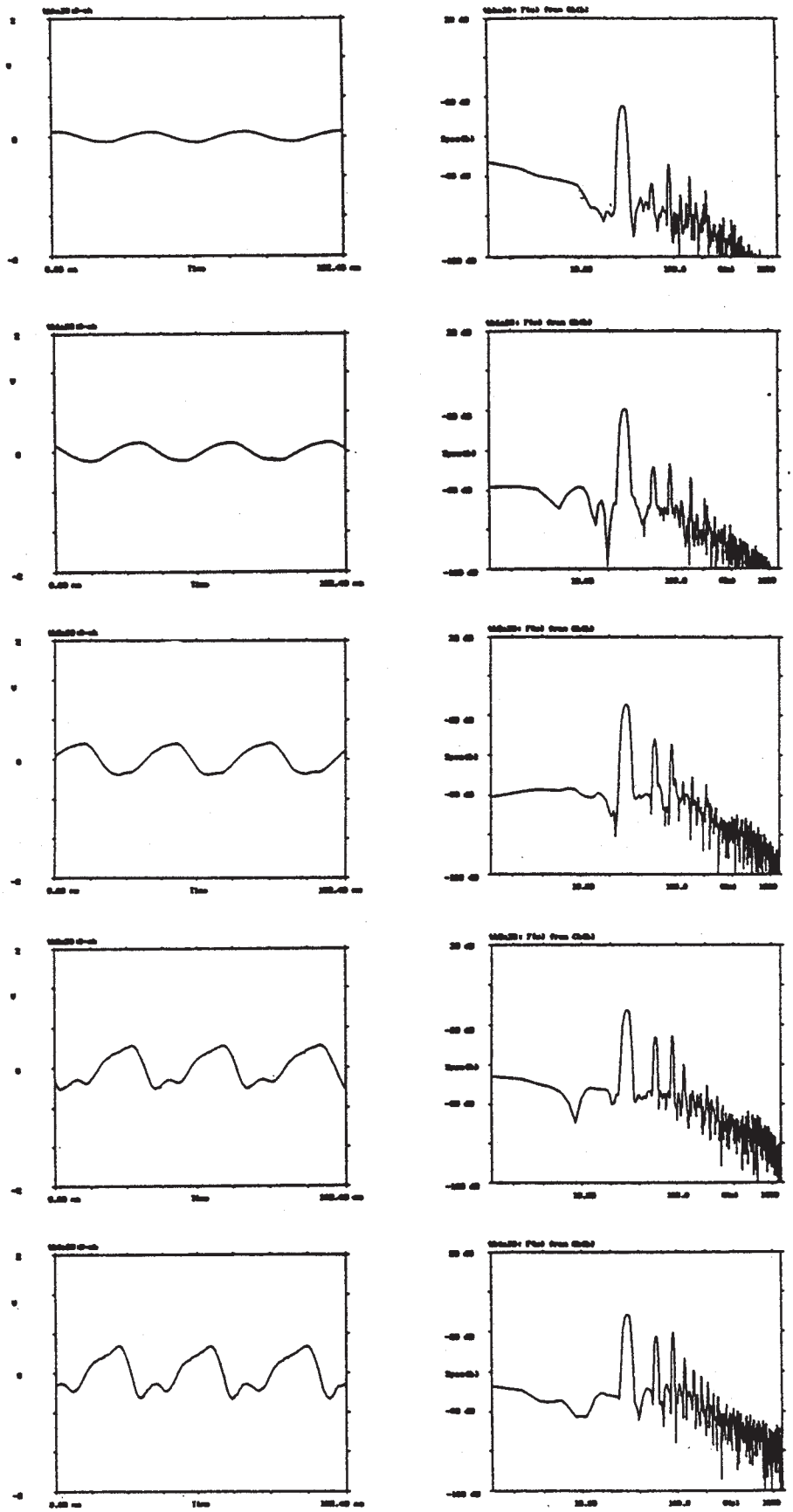

Fig. 14. Waveform data and FFT analysis at increasing levels from a straight flanged port. *Note*: Waveform is triangular and asymmetrical. (From Vanderkooy [3].)

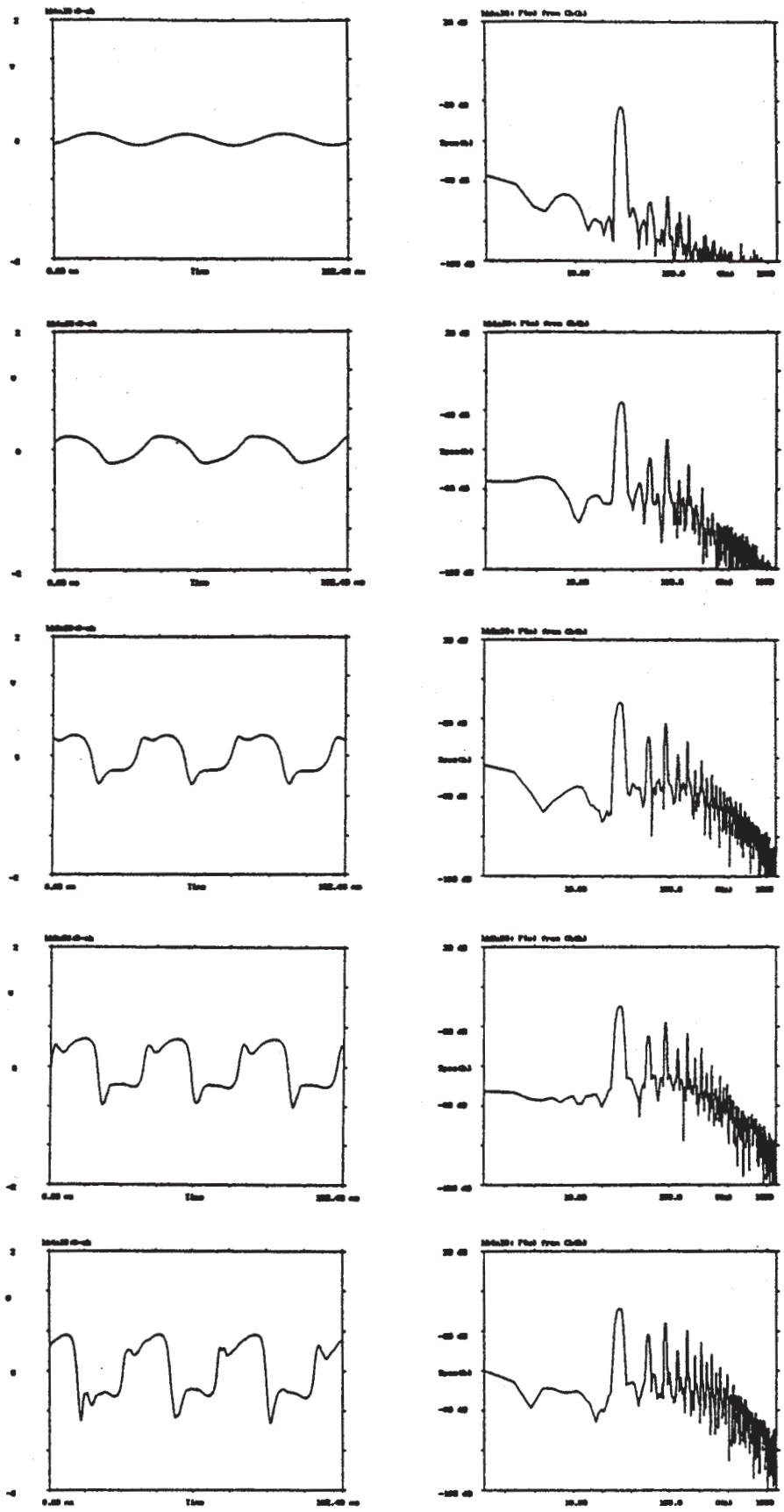

Fig. 15. Waveform data and FFT analysis at increasing levels from a radiused (at both ends) flanged port. *Note*: Waveform approaches a square wave. (From Vanderkooy [3].)

where ρ is the density of air and v is the velocity, to

$$\nabla \cdot \tilde{v} = 0. \tag{2}$$

For air at standard temperature and pressure, this is a valid assumption when the velocity is less than the commonly accepted limit of the Mach number, Ma < 0.3, or a velocity of less than about 100 m/s. This is the case for all loudspeaker applications.

The definition of a Newtonian fluid is that forces due to viscosity are proportional to the rate of deformation. Air and water are Newtonian. Toothpaste is non-Newtonian because one must apply a large amount of force to get the flow started, but then it flows easily. The primary parameter used to describe the behavior of all Newtonian fluids is the dimensionless Reynolds number Re. For flow in a circular pipe, the pipe Reynolds number is

$$\mathrm{Re_d} = \frac{\rho v D}{\mu} = \frac{\text{inertial forces}}{\text{viscous forces}} \tag{3}$$

where D is the pipe diameter, μ is the viscosity of air, and v is the velocity of flow.

In oscillating flows the dimensionless Strouhal number St is also important and is defined as

$$\mathrm{St} = \frac{\omega L}{v} = \frac{\text{frequency}}{\text{mean speed}} = \frac{\text{port radius}}{\text{particle displacement}} \tag{4}$$

where ω is angular frequency and L is the characteristic length (that is, the port radius). According to Peters et al. [14], the values of St ≤ 1 lead to flow separation, vortices, and jets.

Flow can be laminar or turbulent, with the commonly accepted transition between the two occurring near $\mathrm{Re_d}$ = 2300 for pipes. This value is accurate for commercial pipes, but the critical Reynolds number can be much higher if the pipe has flared ends or smooth walls. For example, even for a rather large 4-in (102-mm) port tube this would predict that turbulence would commence at velocities above 0.35 m/s, a very low velocity indeed. A practical upper limit for the Reynolds number obtainable in loudspeaker ports is on the order of 100 000.

Turbulence can be defined as an eddy-like state of fluid motion where the inertial vortex forces of eddies are larger than other forces, such as viscous or buoyant forces, which arise to damp out the eddies. It leads to random fluctuations in the flow velocity, with amplitude variations of up to 20% of nominal and with a wide frequency bandwidth of "noise" components up to 10 kHz. Physically, turbulence occurs when viscous forces are unable to damp out the nonlinear inertial vortex forces $\tilde{v} \times \tilde{\omega}$ that arise in the pipe. Fig. 17 illustrates viscous pipe flow. The flow is to the right, and the vortex rings appear clockwise, facing downstream. Note that the direction of the vortex forces is inward, and these are balanced by the viscous forces, which are directed outward. This equilibrium is delicate and can be upset as the velocity increases. Beyond a critical value of $\mathrm{Re_d}$ any small perturbation will cause the formation of eddies that are too large to be damped. These tiny eddies will cause other eddies to form in the opposite direction, which will then pair up. The swirling eddy pair will similarly lead to other eddy pairs, two of which will pair, and so on, from small scale to large, growing larger until the entire pipe is full of eddies of all sizes and the flow is fully turbulent.

At high Reynolds numbers viscosity can generally be neglected except in the thin layer of fluid that forms along solid boundaries which is aptly called the boundary layer. Here viscous effects are significant. The velocity profile across the boundary layer varies from zero (there is no slip between the boundary and the layer of fluid immediately adjacent) to 99% of the free stream velocity at the edge (see Fig. 18). The typical width of a boundary layer in

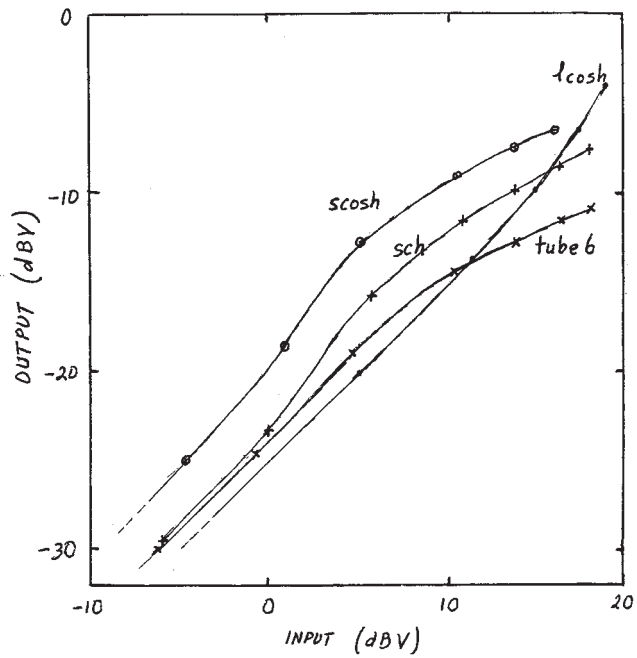

Fig. 16. Output versus input of several flared ports. Note gain before compression. (From Vanderkooy [3].)

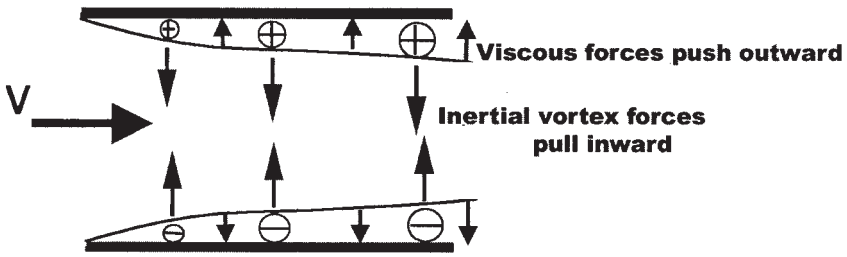

Fig. 17. Balance between viscous forces and internal vortex forces.

ports is on the order of 1 mm.

When the fluid boundaries converge, such as through a nozzle, the flow is essentially squeezed down into a smaller area. The velocity increases and the pressure decreases. This is called a *favorable pressure gradient*, which occurs at the inlet of a flared port. When the boundaries diverge, such as the exit of a gently flared port, a so-called unfavorable or *adverse pressure gradient* is generated where the fluid is forced to lose velocity and gain pressure as the boundary layer hugs the wall. If the flare is too extreme, however, the deceleration of the flow is too great and causes the shear stress at the wall to approach zero. If this happens, the flow runs out of momentum at the boundary and local flow reversal occurs.

As shown in Fig. 19, when the momentum goes to zero, the pressure gradient becomes so large that undesirable flow separation occurs along with the localized reversal. Theoretically this separation of the acoustic flow leads to output-robbing vortices, which sink the acoustical energy into the kinetic energy of the vortex. This energy is then uselessly dissipated by friction instead of acoustic propagation [14]. Note that this situation cannot occur in the other half of the period, when the flow is going in the opposite direction, because flow separation cannot occur when there is a favorable pressure gradient.

Boundary layers may be laminar or turbulent. Turbulent boundary layers have the desirable quality of being able to withstand higher pressure gradients without becoming separated. This is because the turbulent layer has larger wall shear stress and higher momentum near the wall. This extra momentum near the wall allows a turbulent layer to withstand the unfavorable pressure gradient without separation. How does one cause the boundary layer to become turbulent? Some of the factors that would tend to cause transition to turbulence include free stream disturbances, boundary roughness, pressure gradients, or vibration. Obstructions in the boundary layer also hasten the onset of transition to turbulence.

Some experiments performed by Merkli and Thomann [15] found that for oscillating flow, turbulence does not occur over an entire cycle. Rather it occurs in the form of periodic bursts followed by "relaminarization" during the same cycle. They plot that the factor

$$A = \frac{2v}{\sqrt{\mu\omega/\rho}} \tag{5}$$

and found a critical value A_c = 400 above which transition into turbulence occurs. Their study was limited to the frequency range away from the resonance of the pipe ($1.1 < f/f_{res} < 0.9$), whereas we are mainly interested in the frequency near resonance, where the acoustic port output is greatest.

The vorticity Ω is defined as the curl of the velocity vector. Physically it is equivalent to the rate of angular deformation. If $\nabla \times \tilde{V} = 0$, then there is no angular deformation in any plane at any point. The circulation Γ is defined as $\Gamma = \oint \tilde{V} \bullet \mathrm{d}l$. Physically, circulation is the flux of vorticity. If $\Omega = 0$, then the flow is irrotational. This is the case outside the boundary layer if we neglect the Coriolis force and gravity. The boundary layer is definitely not irrotational. These assumptions simplify the momentum equation to the unsteady Bernoulli equation.

To make a detailed analysis of the airflow in a port and develop a design approach it is important to understand the fluid flow dynamics in both directions. The preferred geometry for each may be in conflict as the intake stroke would be well served with a large radius providing a slow head loss and a favorable pressure gradient, and the exit would be well served with a more gradual flare to avoid an excessive adverse pressure gradient.

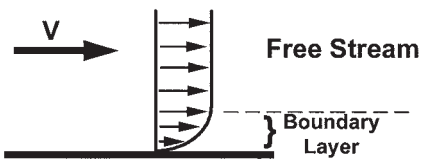

Fig. 18. Velocity profile near a stationary wall.

3 TEN STUDIES

3.1 Power Compression on Straight versus Radiused Ports

The first study undertaken by the authors several years ago was simply to make a side-by-side comparison of the power compression of a straight versus a radiused port. Previous work by Gander [16], Harwood [1], and Young [8] clearly pointed out that all ports do power compress at high levels. As mentioned before, radiused ports have become something of a fashion, and the authors intuitively concluded that they should also have superior fluid flow properties, at least on the inlet air stream, and subsequently less compression. Figs. 20, 21, and 22 show the compression versus the level for a straight 6-in (152-mm)-long, 3-in (76-mm)-diameter port and for the same port with large radii on the inside and outside. The different plots are at different frequencies of 25, 30, and 35 Hz. The port was driven by two 12-in (305-mm)-high excursion

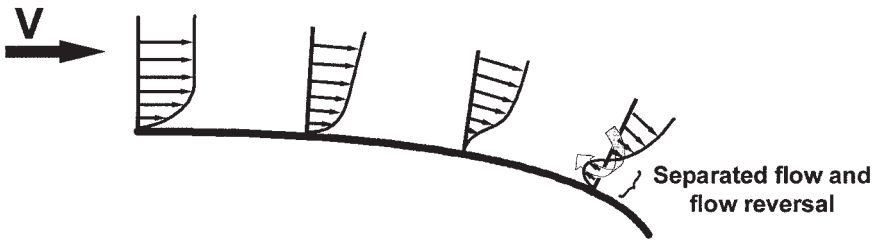

Fig. 19. Adverse pressure gradients can lead to flow separation.

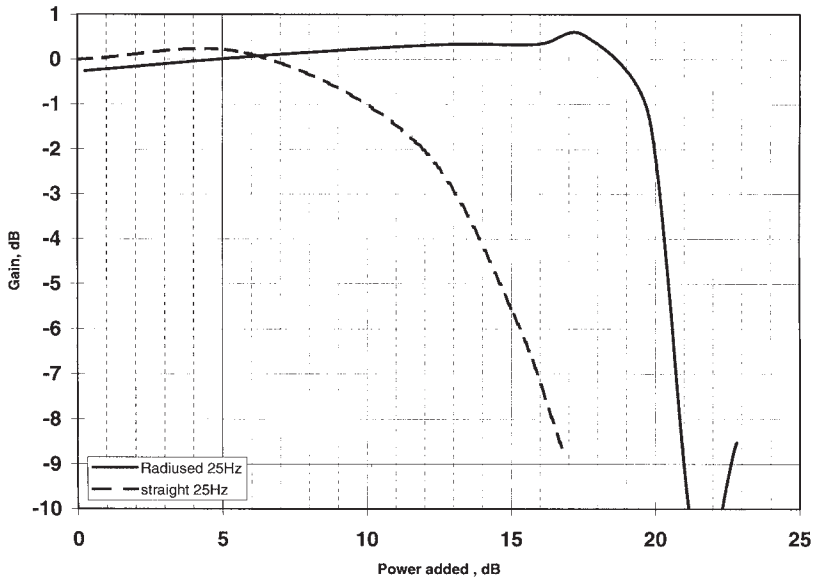

Fig. 20. Compression of 3-in (76-mm)-diameter 6-in (150-mm)-long straight port versus highly radiused port at 25 Hz. Note gain before compression.

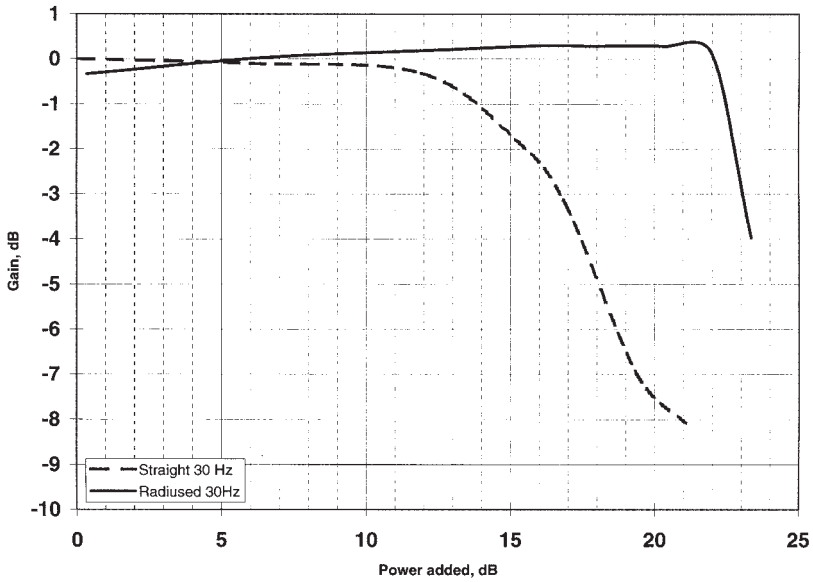

Fig. 21. Compression of 3-in (76-mm)-diameter 6-in (150-mm)-long straight port versus highly radiused port at 30 Hz.

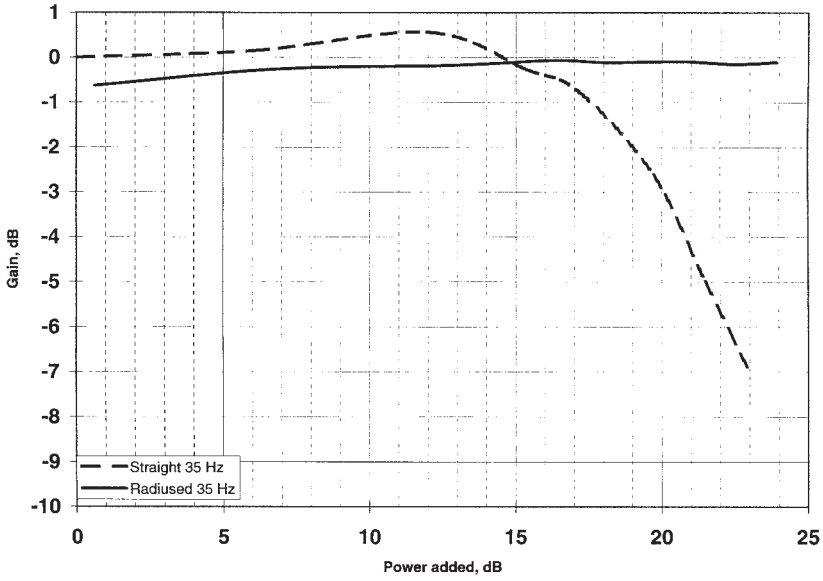

Fig. 22. Compression of 3-in (76-mm)-diameter 6-in (150-mm)-long straight port versus highly radiused port at 35 Hz. *Note*: Velocity is too low to compress radiused port at 35 Hz.

woofers in a 2-ft³ (57-l) box. The tuning frequency was about 30 Hz. The input voltage and current were monitored to account for thermal compression effects, and the output was plotted versus the actual input drive power. The microphone was a small ¼-in (6-mm) B&K microphone spaced about 4 in (101 mm) from the port on axis. This was determined not to interfere with the airflow yet give a high enough port-to-driver output ratio that good results could be seen. A number of observations can be made from this simple experiment.

The first and most obvious observation is that the radiused port compresses substantially less at moderate levels of operation than the straight port. Also at lower frequencies (higher velocities) the effect is much more pronounced. There appears to be a "wall" beyond which neither port is able to go. The conclusion is that this wall exists at the point where the air in the port becomes completely turbulent. Another observation is that about 8-dB more output can be obtained before significant compression sets in. A close examination of the curves suggests an increase or expansion in the medium area of operation of 0.5 dB or so. This implies that at moderate levels the radiused port might have a small boundary-layer separation, which acts as "air bearing" and actually reduces losses in the port.

Most of these conclusions are basically correct but need some adjustment. Previous work by Strahm [17], following Young [8], show that the minimum impedance at port resonance rises as a port compresses. This means that the power delivered to the loudspeaker will go down even if the drivers do not thermally power compress. Since the plot is based on the real power to the drivers, and the straight port begins to compress very early on, the impedance will rise and the compression will appear to be worse. The rise in output in the middle range was also witnessed by Vanderkooy [3], confirming these data. The bottom line is that the difference between the two may not be as great as this experiment suggests, but the radiused port is still much better. Nevertheless, the issue is clearly velocity related, and boundary-layer separation is quite possibly involved at lower levels.

3.2 Port Compression versus Reynolds Number

The previous study and the historical work suggest that port performance and maximum output capability are related to the velocity in the port. In the process of working toward developing ports with optimum performance, the next step is to confirm that turbulence is in fact the culprit and to develop a simple measurement of when that turbulence is too great for desirable acoustical performance.

This study involved the measurement of the velocity of the airflow in three large subwoofers with two 18-in (457-mm) drivers in each. A hot-wire anemometer was placed in the center of the port of three very different port designs. The SPL was again measured with a small ¼-in (6-mm) microphone a few inches from the port. Of the enclosures tested, one had a large single rectangular port, one had three circular ports, and one had four rectangular ports. None had any radii. The area of each port was different in each case, the boxes were tuned differently, and each had different volumes. The question was, what figure of merit could be applied to all subwoofers that would clearly show a relationship to power compression, which would be independent of design?

The conclusion was to take data on the velocity in the middle of the port. The velocity measurements would then be converted to a Reynolds number using Eq. (3) for each of the designs and then plotted versus compression. Figs. 23, 24, and 25 plot compression versus Reynolds number for each of the designs. What stands out is that, for the most part, all three designs show very similar compression curves at all frequencies tested. All designs seem to hit a wall near a Reynolds number of about 50 000–100 000. This number was also confirmed by Vanderkooy [3]. The Moody chart, a standard reference chart used in fluid mechanics, shows the relationship between the Reynolds number and the turbulence in pipes (Fig. 26). It can be considered to have three regions: laminar, turbulent, and a region of transition between the two, shown shaded in the figure. The range of Reynolds numbers given here falls in the transition zone. The conclusion is that compression is clearly related to turbulence and that a Reynolds number of about 50 000 is a good indicator of when the system begins to degrade.

3.3 Modeling Flared Ports and Prediction of Tuning

Everyone, from piping system engineers to carburetor designers, knows that pipe entrance losses are highly dependent on the geometry. Interestingly, exit losses are independent of geometry. However, audio signals by definition are oscillating, and therefore both sides of a loudspeaker port are "entrances" and would benefit from rounding of the edges. A well-rounded entrance with a radius of 20% of the pipe diameter yields a very low 5% loss, whereas a sharp entrance asymptotically reaches a 50% loss (Fig. 27).

The main difficulty in modeling flared loudspeaker ports is the infinite variety of profiles that will yield the same port tuning. Many loudspeaker designers choose not to experiment with flared ports because without a well-defined diameter to plug into the standard port tuning formula, they are left to design by trial and error. There are no CAD programs that incorporate the ability to design flared ports as of yet. However, there is a growing demand to take advantage of flared ports and a need for predicting their performance.

The tuning of a port, flared or otherwise, is a function of the ratio of the port cross-sectional area to the port length. For a standard straight cylindrical port, and neglecting end corrections, there are several equivalent embodiments of the port tuning equation:

$$f = \frac{1}{2\pi}\sqrt{\frac{\gamma P_0 A}{\rho V_b L}} = \frac{c}{2\pi}\sqrt{\frac{A}{L V_b}} = \frac{c}{2\pi}\sqrt{\frac{\rho}{m_{ap} V_b}} \qquad (6)$$

where $\gamma = 7/5$ for air, P_0 is the ambient atmospheric pressure (101 000 Pa), ρ the density of air (1.2 kg/m³), A the port cross-sectional area, V_b the box volume, L the port length,

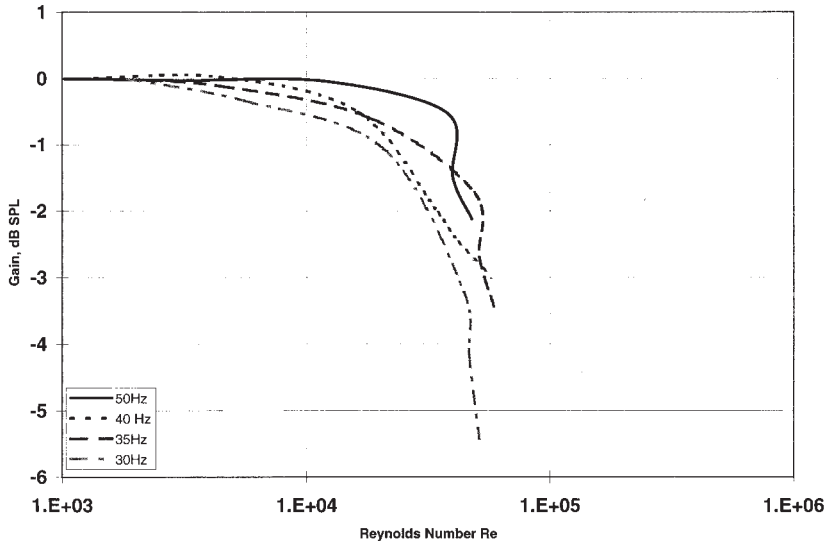

Fig. 23. Port compression versus Reynolds number in double 18-in (457-mm) subwoofer, 10 ft³ (0.28 m³), tuned to 45 Hz with a single rectangular port.

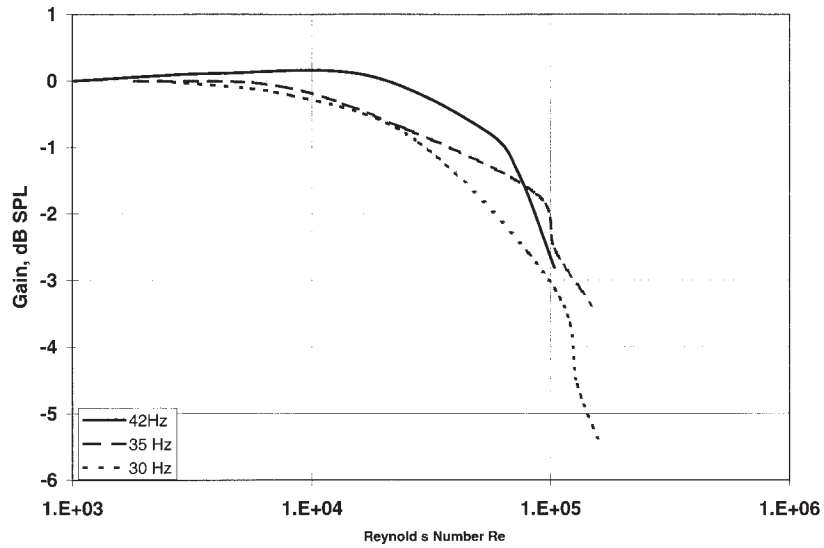

Fig. 24. Port compression versus Reynolds number in double 18-in (457-mm) subwoofer, 12 ft³ (0.34 m³), tuned to 35 Hz with three straight round ports.

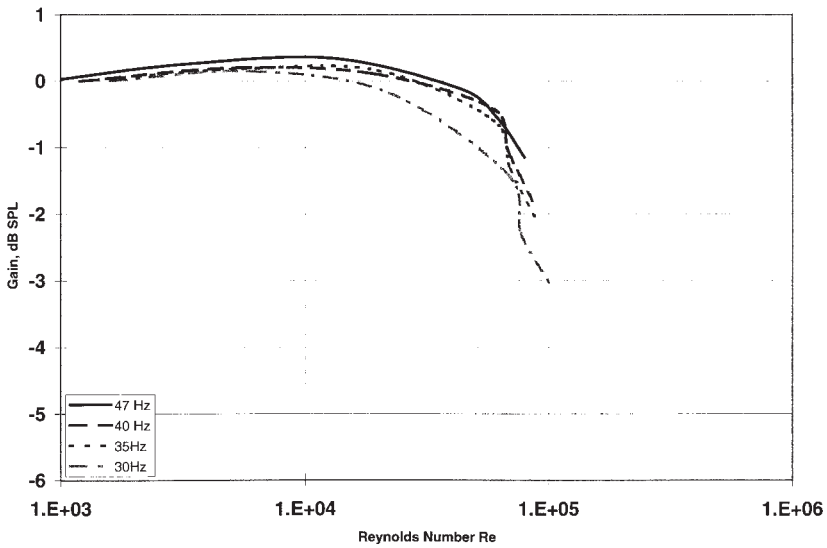

Fig. 25. Port compression versus Reynolds number in double 18-in (457-mm) subwoofer, 12 ft³ (0.34 m³), tuned to 39 Hz with four straight square ports.

and m_{ap} the acoustic mass of air in the port.[2] Notice that the A/L ratio enters directly with other nonport parameters.

For the generalized cause of ports with arbitrary cross sections, one only needs to find the effective A/L ratio to which simplifies to

$$m_{ap} = \frac{\rho L_{eff}}{\pi a^2} \tag{8}$$

for a standard cylindrical port.

[2] The acoustic mass reactance in the port m_{ap} in units of kg/m^4, is given by

$$m_{ap} = \int_{-L/2}^{L/2} \frac{\rho}{A(x)}\, dx + E_c \tag{7}$$

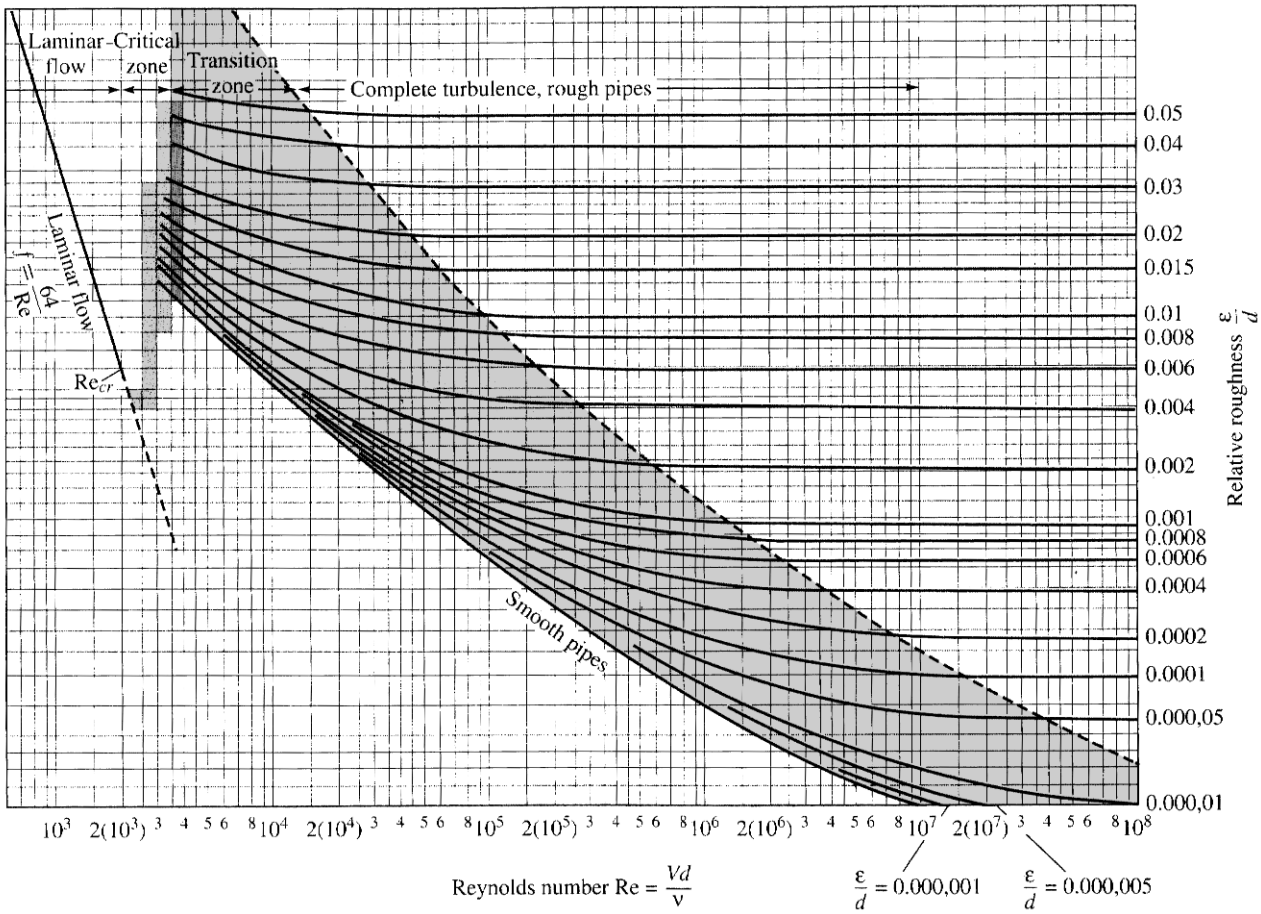

Fig. 26. Moody chart showing relationship between Reynolds number, turbulence, and roughness. (Adapted from White [18].)

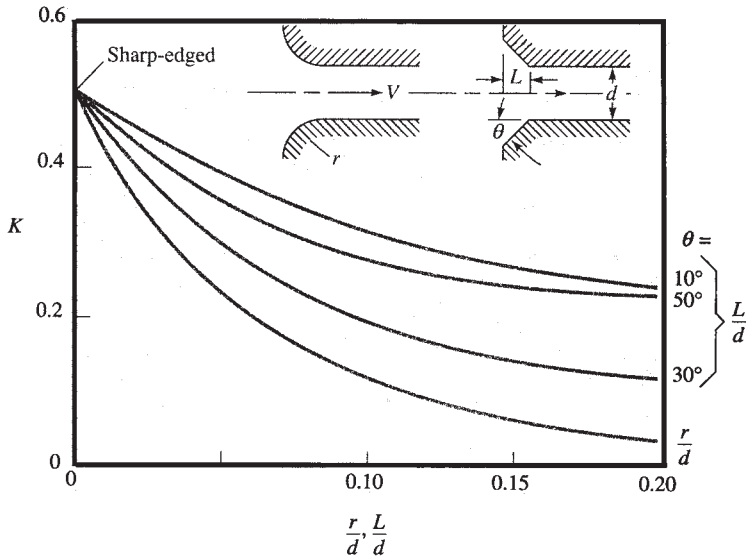

Fig. 27. Entrance loss coefficients for rounded and beveled inlets. Lower curve applies to rounded geometry. K—loss coefficient related to ratio of pressure drop to velocity. *Note*: $r/d = 0.2$ yields a nearly lossless inlet. (From White [18].)

find the actual tuning frequency. Vanderkooy has shown the formula for this to be

$$\left[\frac{A}{L}\right]_{\text{eff}} = \frac{1}{\int_{-L/2}^{L/2} \mathrm{d}x/A(x)} + E_{\text{c}} \tag{9}$$

where $A(x)$ is the area function and E_{c} any end correction. The difficulty for flared ports arises in finding the correction E_{c}. End corrections are needed because the radiation impedance of a port is not zero, the free ends of which act as a vibrating diaphragm. However, since the radiation impedance is small, the effect is merely to increase the effective length of the tube by an amount δ. For traditional straight ports, δ is a well-known quantity, equal to $0.61a$ for a free end and $0.85a$ for a flanged end, where a is the port radius [19, p. 131]. For straight ports δ is relatively constant over a wide range of driving amplitudes.

Flared ports, however, do not have a well-defined diameter, and so δ is not so simple. In effect, the end correction is a measure of the inertia of the flow at the exit. Given that each port shape has a different correction, is there any hope of developing a generalized port tuning equation? Some method of approximating a general port flare would need to be devised so that the effect of the "amount of flare" could be studied. For simplicity, we chose to investigate flare profiles described by a simple radius. Using this simplification we can define a *normalized flare rate* (NFR) as the ratio of overall port length to flare radius,

$$\text{NFR} = \frac{\text{port length}}{2(\text{flare radius})}, \qquad 0 < \text{NFR} < 1. \tag{10}$$

Thus a straight port would have an NFR of 0.0, and a very extreme port with a full radius would have an NFR of 1.0 (Fig. 28). Most port profiles can be approximated with an NFR in this range. This normalization of scale allows the results to be generalized to any port size.

An initial sample of six port tubes, all of 120-mm length and a minimum diameter of 60 mm, were made with NFRs of 0, 0.125, 0.25, 0.5, 0.667, and 1.0. In addition, all profiles had a small 12-mm blend radius on both ends to avoid sharp edges, as well as a 140-mm outside-diameter inner baffle for symmetry (Fig. 29).

Unexpectedly the port tuning frequency was only weakly dependent on the amount of flare. Clearly, the port length and minimum throat diameter appear to be the main determinates of tuning. As the port flare becomes more pronounced, the end correction, as typically calculated based on the radius at the mouth, overestimates the reactive air mass present. A better way to predict tuning appears to be basing the length correction on the minimum throat diameter instead of the maximum diameter. Following this path, fitting the experimentally determined tuning frequencies to a function of the flare radius leads to a striking linear relationship ($r^2 = 0.98$) between NFR and the effective port area (Fig. 30). The data fit yields port tuning predictions within 2% for all six ports, and within 5% for all other port profiles tested subsequently, including elliptical and exponential profiles. Of course, the accuracy of prediction is better the closer a given profile can be approximated by a simple radius. The formula is

$$f = \frac{c}{2\pi}\sqrt{\frac{A_{\text{eff}}}{L_{\text{eff}} V_{\text{b}}}} \tag{11}$$

where

$$A_{\text{eff}} = \underbrace{\left[1 + 0.576\left(\frac{L_{\text{act}}}{2r_{\text{fit}}}\right)\right]}_{\text{NFR}} A_{\text{min}}$$

$$L_{\text{eff}} = L_{\text{act}} + D_{\text{min}} \ .$$

Here c is the speed of sound, L_{act} the actual port length, r_{fit} the best fit flare radius, A_{min} the minimum throat area, D_{min} the minimum throat diameter, and V_{b} the net box volume.

The only difficulty in using this formula is finding the best fit flare radius to a given profile. But even this is relatively easy using the built-in optimizers in most spreadsheet software.

3.4 Acoustic Compression

As the SPL of a port is increased, there is no escaping some degree of port compression. The question becomes, how the port flare affects this compression, if at all. As described previously, turbulence is most likely the culprit. One effect of turbulence in a port is a reduction of the Q of the resonance. This causes a drop in the acoustical output at resonance.

In order to explore this phenomenon, another test enclosure was constructed using a 1-in (25-mm) MDF with a single high-throw 18-in (457-mm) woofer. The bandpass box had a ported chamber volume of 201 l and a sealed chamber volume of 111 l. Testing conducted with this

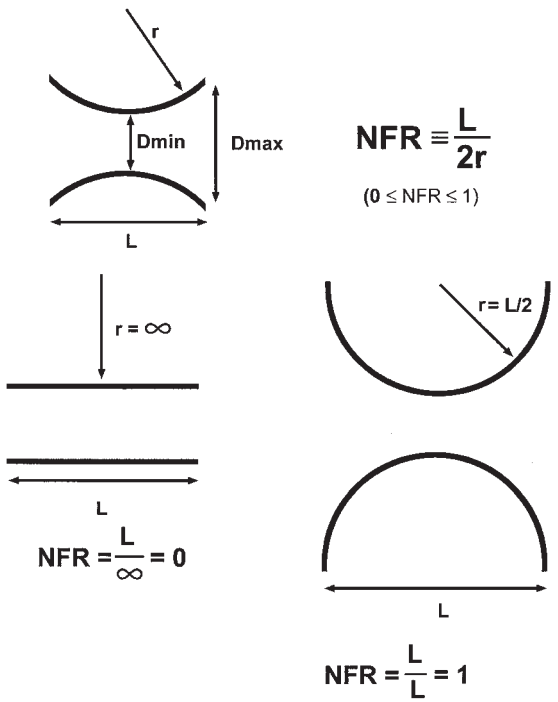

Fig. 28. Simple radiused port nomenclature.

box would effectively remove acoustic contributions from the transducer (as it is buried within the box), leaving only the port output. The box loss Q_L was measured by the Thiele method at over 14, indicating a very rigid, low-loss box.

Initial trials were made to find the best microphone placement for measuring compression (see Pedersen and Vanderkooy [13] for an extensive investigation). The pretrials were conducted with the microphone at the port mouth, inside the box, and at 2 m measured on a ground plane (Fig. 31). The data showed that the compression measurements are very similar in all cases, yet the cleanest data came from the in-box measurement, so this method was chosen for subsequent experiments. In-box acoustic measurements were performed using a B&K 4136 ¼-in microphone, which has a 3% distortion limit of greater than 170-dB SPL. To prevent transducer power compression from contaminating the results, a very high-power driver with minimum power compression in the test range was employed. The transducer was driven using a large power amplifier in the bridged mode, which can provide 2 kW of output into 4 Ω. Most measurements were made over a frequency range of 10–100 Hz using a 15-s sweep from low frequency to high. Each port was driven

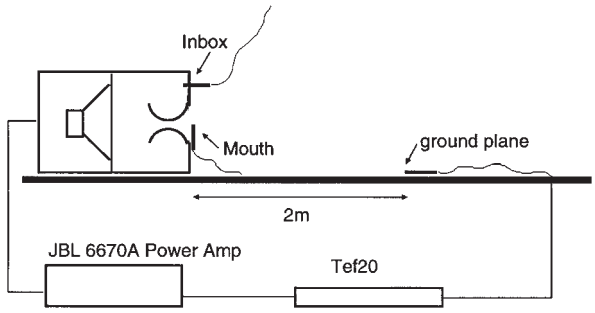

Fig. 31. Bandpass loudspeaker setup for compression testing. Before selecting the "in-box" position for all compression measurements, the three microphone locations shown were tried.

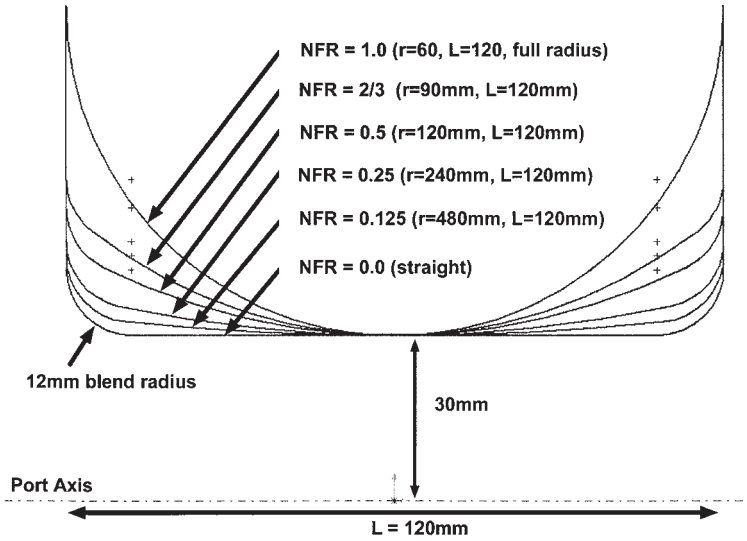

Fig. 29. Port profiles for study.

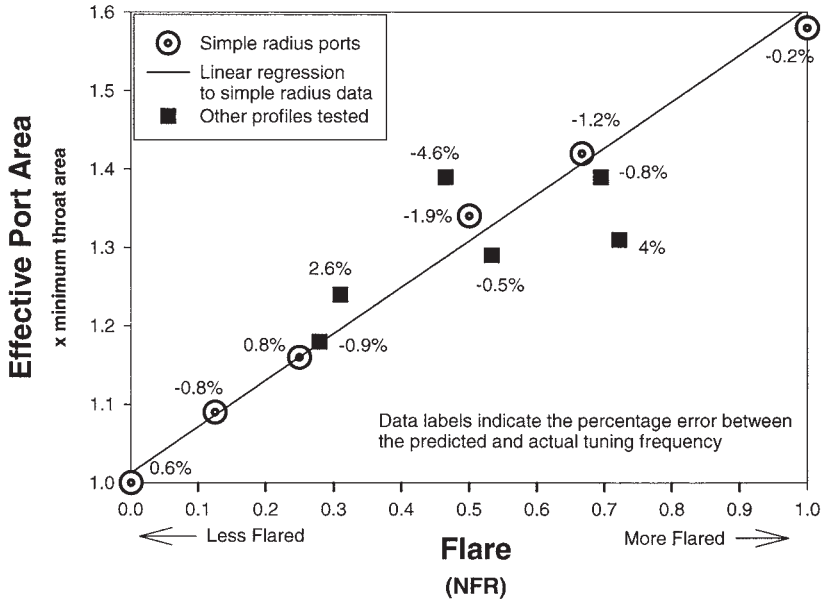

Fig. 30. Curve fit of flare rate to port tuning data.

at successively higher voltages in 6-dB increments beginning at 1.25 V and ending at 40 V. The curves were then mathematically lowered by the amount the input power was increased so that they would overlap, except for the compression effects. The results from some representative ports are shown in Figs. 32–35. They indicate that there is no compression at the end of the sweep, so we can be sure that all compression shown is solely due to the port. Despite the fact that all ports compress, the ways they compress appears to differ. The largely radiused ports not

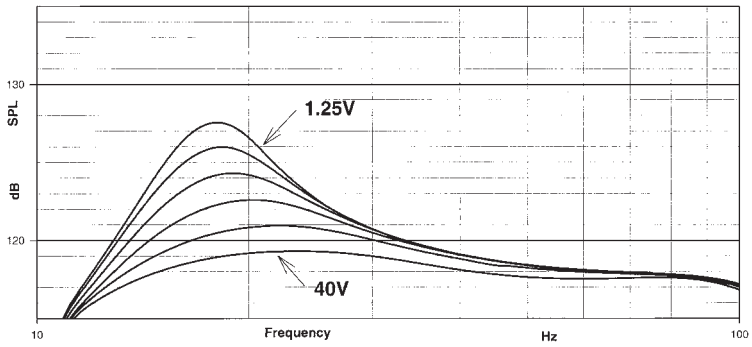

Fig. 32. Port compression measured in box for port with NFR = 0.0; 6-dB voltage increments from 1.25 to 40 V rms. Each progressive curve was lowered 6 dB. Since all curves overlap at higher frequencies, no thermal compression is evident, and all curve differences are due to acoustic compression.

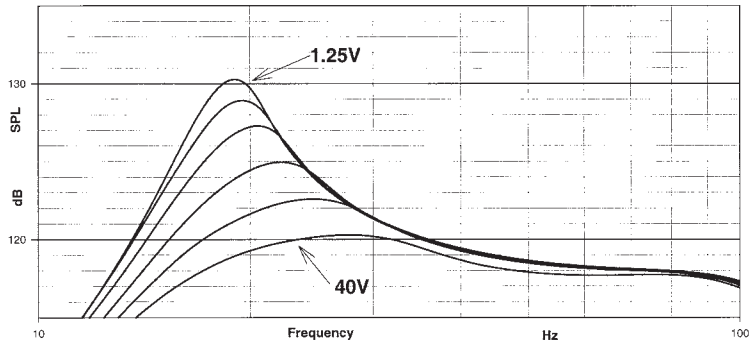

Fig. 33. Port compression measured in box for port with NFR = 0.25.

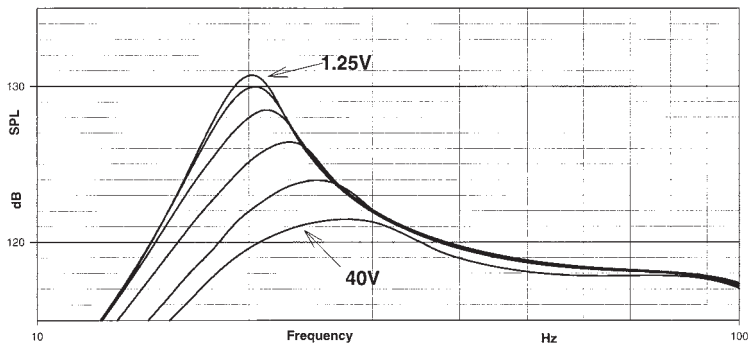

Fig. 34. Port compression measured in box for port with NFR = 0.5.

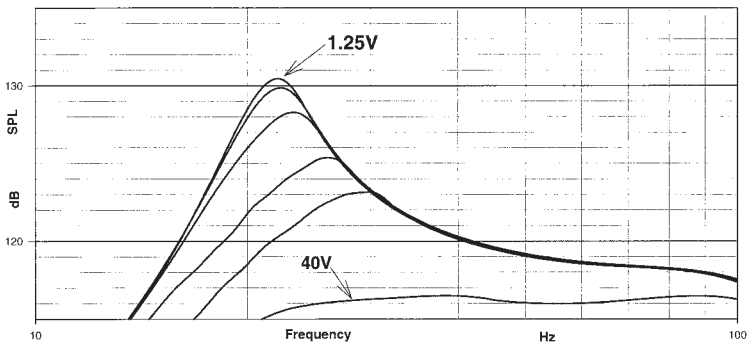

Fig. 35. Port compression measured in box for port with NFR = 1.0.

only compress in level, but the frequency of the resonance shifts also. It is suspected that this happens because the port becomes effectively shorter as it starts to become turbulent, confirming Vanderkooy's contention that the end correction changes with the level. The section of the port area near the end has severe boundary separation due to the adverse pressure gradient, as predicted by Roozen et al. The air in this section is largely turbulent and is not part of the acoustic mass of the port. The port is thus effectively shorter and tunes higher. Of additional interest is that the largely radiused ports have a higher output at low levels. The *Q* of the port is clearly higher and losses are less. The straighter ports show less frequency shift, but in the straight ports the compression and losses are relatively high, especially at low levels. An optimum solution strikes a balance between minimizing frequency shift and compression. The port with NFR = 0.5 appears to find this balance.

Fig. 36 shows the same data as Figs. 32–35, but "sliced" vertically at 20 Hz and plotted relative to the straight port, whereas Fig. 37 is taking the maximum value of each curve instead. Either way, all ports measured showed severe compression, on the order of 10 dB at port tuning at the highest power levels. Despite the close grouping of the data, suggesting that any moderate amount of flaring is good and that there is no clear winner, there were some differences noted. The most obvious conclusion is that a large radius is clearly better at lower levels. Also, it appears that the more extreme the port flare, the worse the compression at high levels. In addition, the straight port starts out with about 2 dB less output than any flared port, but it compresses less dramatically than would be expected. A close examination points to a "sweet spot," where a moderate amount of flare (NFR $\approx$ 0.5) works better than all others.

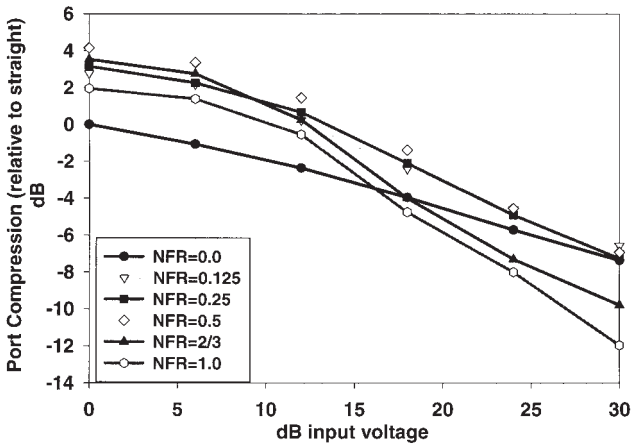

Fig. 36. Port compression versus level at 20 Hz for simple radius ports. *Note*: NFR = 0.5 is best.

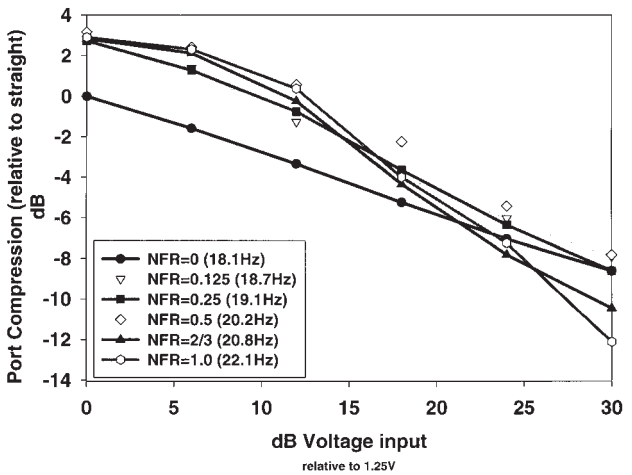

Fig. 37. Port compression at port tuning versus level for simple radius ports. *Note*: NFR = 0.5 is best.

3.5 Distortion Measurements

Probably the single most remarkable characteristic of flared ports as compared to straight ones is the marked reduction in distortion that can be achieved. It is clear that aerodynamic profiles are much quieter than their straight counterparts, but once again we can question whether a particular profile has advantages over any other.

To answer the question, another enclosure was built as a bandpass box, which could be mounted in a 2π anechoic chamber to maximize the signal-to-noise ratio, as shown in Fig. 38. A very long throw 15-in (381-mm) woofer was used to excite the ports. Harmonic distortion was measured using a sine source set to the tuning frequency of each port in the vented test enclosure. MLSSA was used as a digital storage scope to capture several cycles of the acoustic output at a distance of 1 m from the port. The microphone was placed 45° off axis to avoid contamination from jets. A fast Fourier transform was applied to the captured waveform, and the amount of energy at the desired frequency multiples was calculated. The test was

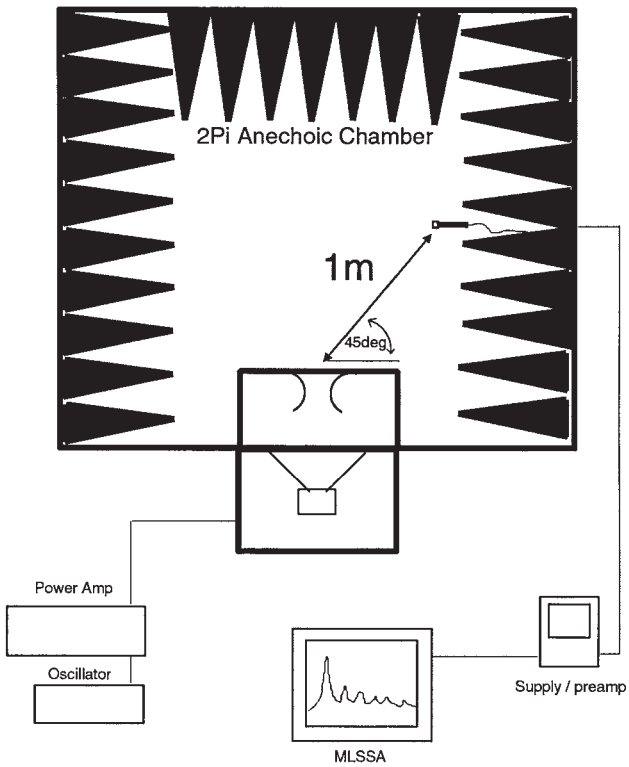

Fig. 38. Distortion measurement setup. A bandpass loudspeaker mounted in a 2π anechoic chamber was used to measure distortion. Note off-axis position of microphone to avoid contaminating data with subsonic noise due to exit jets.

repeated at an increasing input voltage in 1-dB increments until the limit of the amplifier was reached at 40 V. Results were examined for odd harmonics, even harmonics, and total harmonic distortion (THD) (all harmonics). Although noise is the most obvious artifact, nonharmonic noise was not considered for this experiment because early testing showed that port differences are captured well with harmonic analysis (Fig. 39). In all cases, most harmonic distortion occurs in the odd harmonics, with most ports examined having generally low amounts of even harmonics (Fig. 40). Examination of these results shows that port symmetry (that is, adding a flange on the inside port end) is important for minimizing this type of distortion. As expected, a low even harmonic content is found in symmetrical ports. Odd harmonic content, however, is strongly affected by port flare geometry (Fig. 41). Fig. 42 combines both odd and even harmonics into a THD measurement. In these experiments, straight ports are clearly inferior to ports with even the gentlest flare. As to flared ports, the results generally show that at lower acoustic levels, greater port flares yield lower distortion, with the NFR = 1.0 port performing best as it is the least lossy, as shown in Section 3.4.

At higher levels, near 100 dB at 1 m, ports with moderate flare lead the pack, with NFR = 0.5 being optimum.

At very high levels (over 100 dB at 30 Hz from a 2.5-in (63.5-mm) port), however, it is apparent that too much flare causes more distortion than gentler flares. Surprisingly, standard straight ports do not fare as poorly at high levels as would be expected. In fact, very gentle

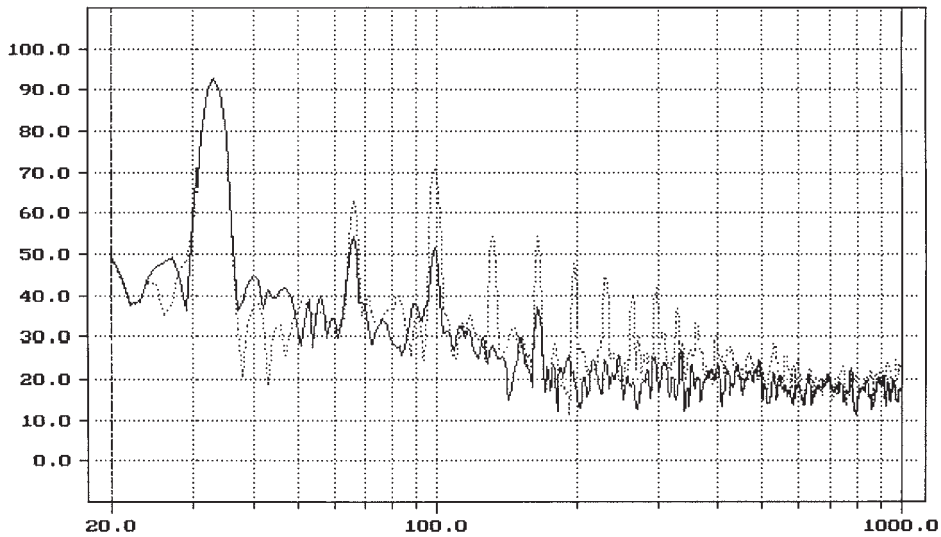

Fig. 39. Spectra of worst port (···) and one of the best ports (—) at 93-dB SPL fundamental of 33 Hz, showing that a THD measurement captures the differences. Noise is well below harmonics; therefore the level of harmonics represents a good measure of the performance.

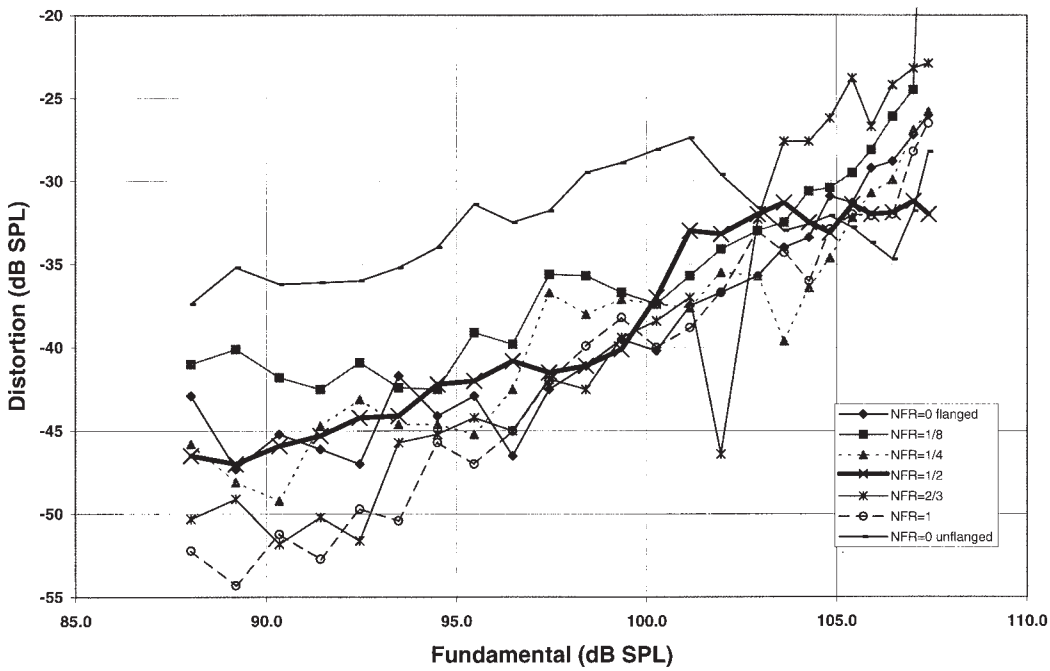

Fig. 40. Even harmonics of some representative ports versus fundamental at increasing SPL.

flares are worse than no flare at all.

There appears to be an optimum. A moderate amount of flare for best *overall* distortion performance is required. This profile is a compromise for best performance over the entire amplitude range. Once again, the optimum normalized flare rate is near 0.5.

3.6 Velocity Measurements and Jet Formation

As discussed in earlier sections, the air velocity in the ports is intimately related to performance. In order to explore the velocity magnitude and distribution across the face of flared ports and to gain a better insight into jet formation, a hot-wire anemometer (TSI model 8360) was used to measure the air velocity across the six ports studied in Section 3.5. Measurements were mainly performed at the mouth in the baffle plane. The velocity profile across each port mouth was measured for increasing input power into a test enclosure, which was a 24-in (243-mm) cube made of 1-in (25-mm) MDF with four 18-in (457-mm)-high power woofers. One side was fitted with a cutout to accept interchangeable baffles. Based on the 2–3-in (51–76-mm) minimum port throat diameter selected, four woofers undoubtedly would be sufficient to create the required volume displacement needed to fully characterize

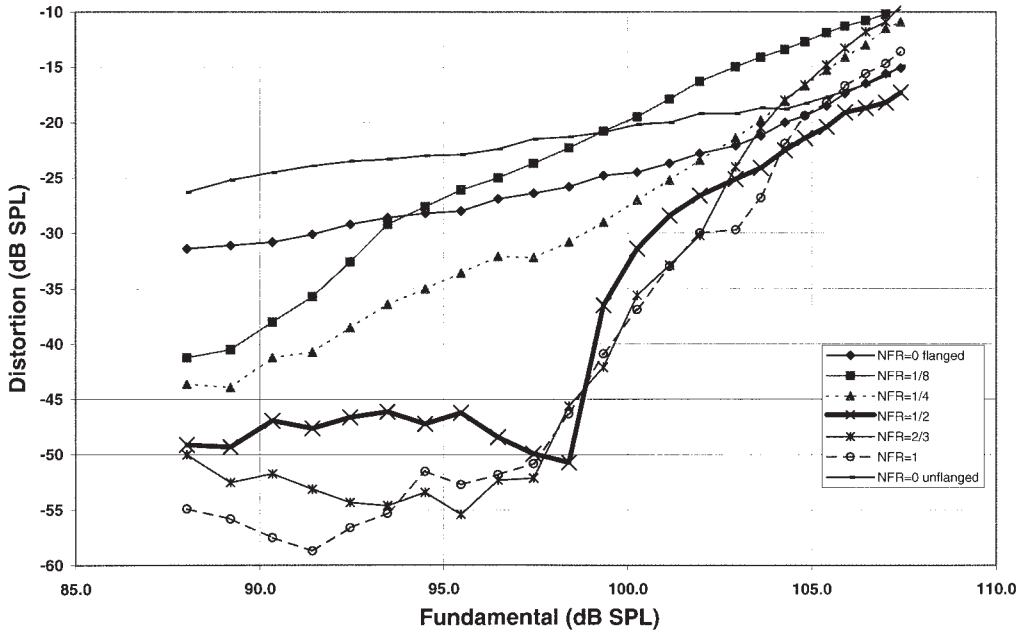

Fig. 41. Odd harmonics of some representative ports versus fundamental at increasing SPL.

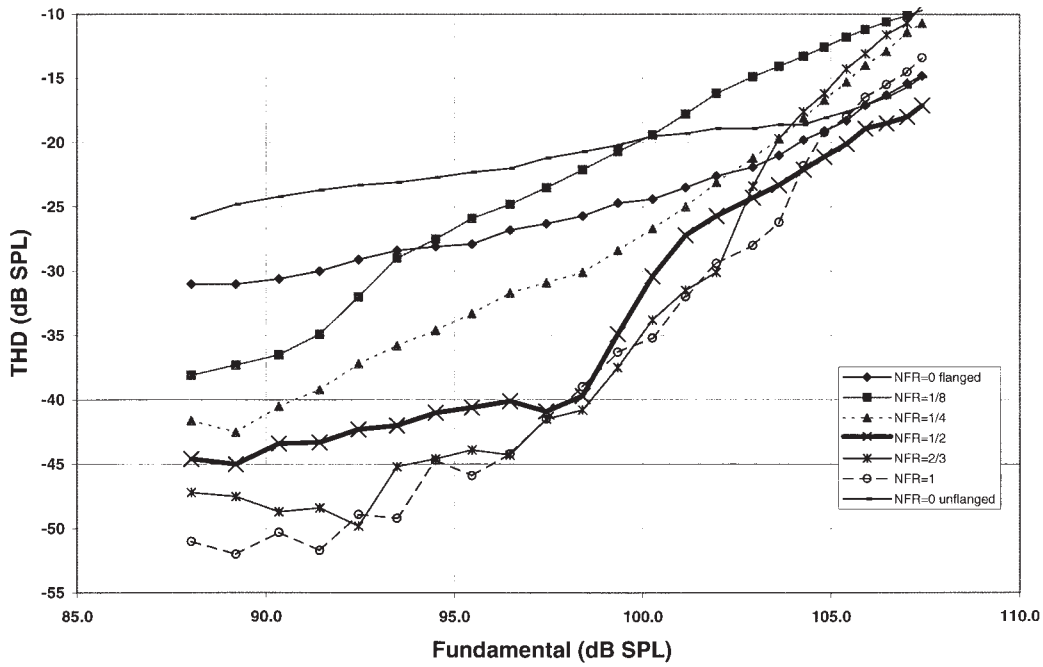

Fig. 42. THD for some representative ports versus fundamental at increasing SPL.

each port for air velocity measurements. The transducers were driven using a large power amplifier in bridged mode, which can provide 2 kW of output into 4 Ω. Measurements were made near port tuning, where the velocity would be greatest. As can be seen in Fig. 43, the measurements tend to confirm previous work, indicating that at low to medium levels the air velocity is greatest near the port walls, and a ring of high velocity is forming lower velocity on the port axis. At high levels, when jets form, however, this behavior is not present, and the velocity magnitude is greatest at the port center. It is interesting to note in Fig. 44 that the straight port and the most gently flared ports have the highest velocities across an area that maps to the center hole diameter; it then rapidly drops off, suggesting a clear jet has formed. They seem to exhibit very similar maximum velocities, and this transition occurs at about 10 m/s, as predicted by Young. On the other hand the most radiused ports have a much more evenly distributed velocity profile, with a lower maximum velocity possible, suggesting more compression as the total area under the curve appears similar. The one port profile that stands out as having the best of both worlds is the port with the 120-mm radius (NFR = 0.5). The "area under the curve" approaches a maximum, suggesting the least amount of total compression and the greatest output. This study also points to a balance of conditions for inlet and outlet airflow preferences in geometry.

3.7 Roughness Experiment

One might think that smoother surface textures in ports would directly result in higher performance. However, since Coulomb's experiments in the 1800s it has been known that the surface roughness has an effect on friction resistance. Interestingly, the effect is negligible in laminar flow, but not if the flow is turbulent, that is, surface roughness effects would be evident only at the higher port velocities. If reduced drag is desired, a rough surface will actually perform better due to boundary-layer effects. This

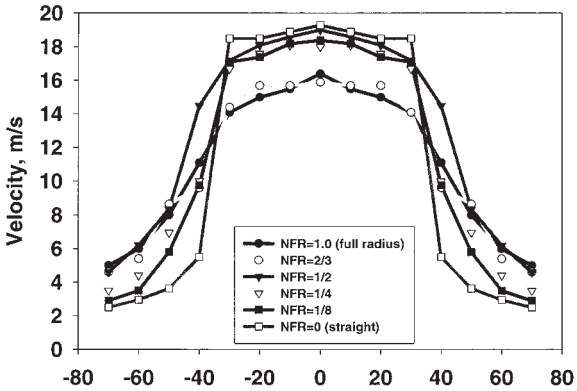

Fig. 44. Velocity profiles at 20 Hz at very high levels for all ports in study.

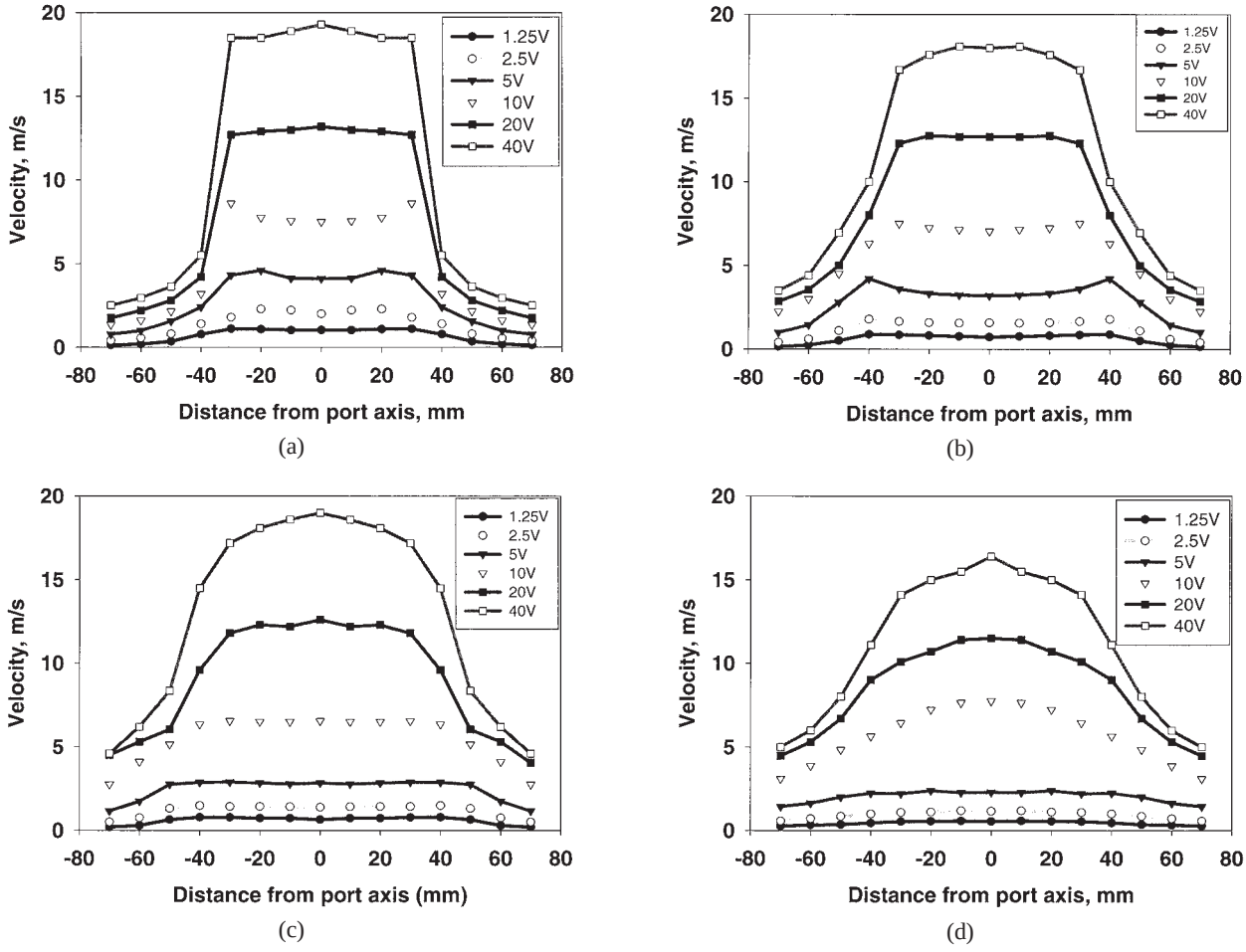

Fig. 43. Port velocity profiles at 20 Hz. (a) NFR = 0.0. Note higher velocity at port edges for 10-V measurement. (b) NFR = 0.25. 5-V measurement shows rise in velocity at edges. (c) NFR = 0.5. Ports with NFR = 0.5 or higher do not show higher velocity at port edges. (d) NFR = 1.0.

is the reason why golf balls have dimples—the surface roughness is intended to "trip" the boundary layer so that it will go turbulent at a lower Reynolds number (in flight the Re of gold balls is about 100 000). The turbulence causes the separation point to move from the front to the back of the golf ball, thereby reducing drag and allowing a farther flight. There are now even commercially available subwoofer loudspeakers that use a flared port with dimples, similar to a golf ball. Fig. 45 shows a bowling ball entering the water at 25 ft/s (7.6 m/s), demonstrating how much larger the wake is on the smooth ball [Fig. 45(a)] versus that of the surface-roughened ball [Fig. 45(b)]. Notice also that the separation point has moved farther back.

Another example of intentionally induced turbulence is often seen on the top surface of airplane wings near the leading edge. These "vortex generators" are used to prevent boundary-layer separation, which could cause the wing to stall under high lift conditions such as during landing.

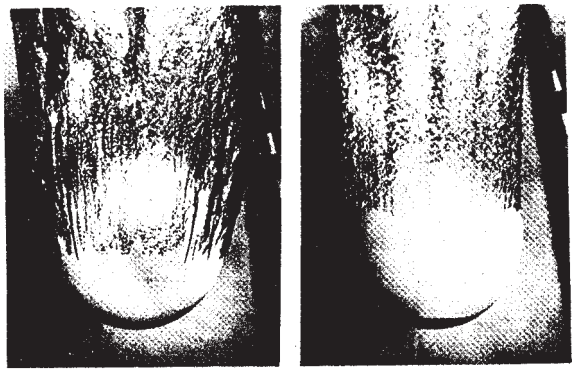

(a) (b)

Fig. 45. Strong differences in laminar and turbulent boundary-layer separation of 8.5-in (216-mm) bowling ball entering water at 25 ft/s. (a) Smooth ball, laminar boundary layer. (b) Same entry; turbulent flow induced by patch of roughness on leading surface. (From [18].)

In fluid mechanics, surface roughness is characterized by the dimensionless roughness ratio:

$$\frac{\varepsilon}{d} = \frac{\text{wall roughness}}{\text{diameter}} . \tag{12}$$

Small changes in the roughness ratio can lead to very large effects in the turbulent flow region. To test the hypothesis, we constructed five copies of the best performing port (NFR = 0.5) and then affixed precision glass beads of various sizes, ranging from 1 to 2.5 mm, to the inside port walls using a spray adhesive. This corresponds to a roughness ratio range of approximately 0.02–0.04. These ports were manufactured such that the volume occupied by the beads was accounted for. The ports were then subjected to the same distortion and compression tests described earlier. Contrary to expectation, over the range of roughness examined, rough ports were generally inferior to the smooth-walled port. Rough ports had more harmonic distortion above 95 dB at 1 m. Only in a very narrow range, between 90 and 95 dB, did the wall roughness produce a marginal improvement in odd harmonic distortion. At all other levels the smooth-walled port performed better (Fig. 46).

Based on the fluid mechanics literature [18], we expected to see a benefit in rough walls in the acoustic compression measurement. Unfortunately, roughened port walls failed to show any advantages here as well. In fact, Fig. 47 shows that all rough ports were consistently compressing about 1–1.5 dB more than the smooth port. These negative results may be explained by noting that even at the highest Reynolds numbers near 100 000, the Moody chart predicts that we are only just entering the transition region and have not reached the fully turbulent region where roughness would be expected to make a large impact. Based on these results, it does not appear that dimpling the walls guarantees any extra performance.

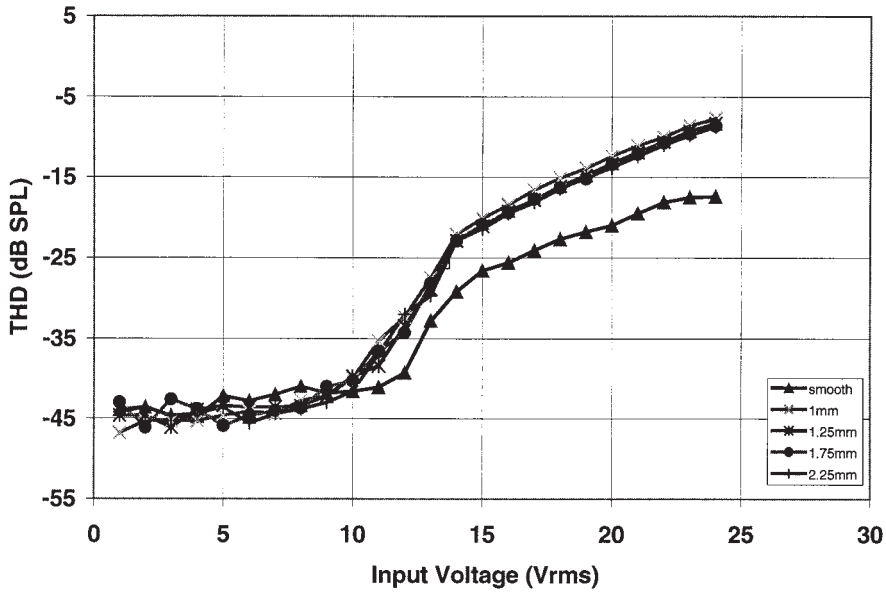

Fig. 46. THD of ports in roughness study. Textured ports performed poorly over most of the testing amplitude range. Differences are mainly due to odd-order distortion (not shown).

3.8 Polynomial Flare Profile

Taking a slightly different approach to defining the flare rate, we chose to use a polynomial expression to define the port profile instead of a simple radius. The idea was to see whether an optimum solution might exist by approaching the problem from a different angle. It was further desired that all ports tune to the same frequency so that this would be a tightly controlled, legitimate comparison. This tuning requirement dictated that the ports have different minimum throat diameters in order to achieve identical m_{ap} values. Recall that all ports from the previous studies had identical minima and therefore tuned differently. A series of seven ports was designed with ratios of maximum to minimum diameter ranging from 1:1 to 2:1. All ports had the same physical length, and a 15-mm radius was added to both ends of each port. For reference a straight port (port s) and an elliptical port (port el), similar to the one cited by Gawronski and Caron [9], were also included in the experiment. Fig. 48 depicts the profile of the ports, and Table 1 completes the description of the ports.

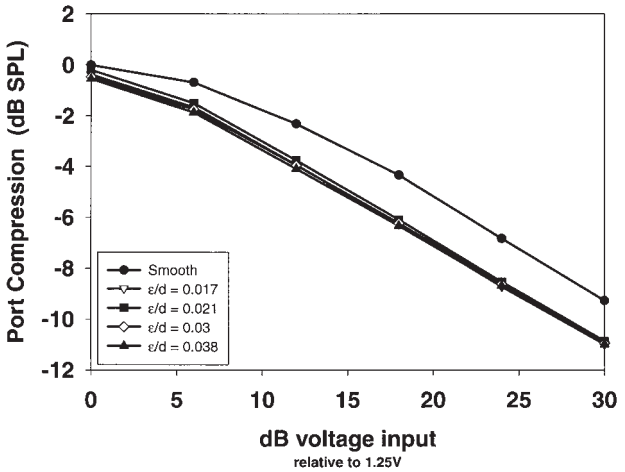

Fig. 47. Port compression of ports in roughness study. All textured ports performed worse than smooth port.

The ports were mounted in the bandpass enclosure described in Section 3.5. The experimental setup follows that of Section 3.5, except that all ports were driven by a 33.0-Hz sine wave with drive levels ranging from 1.12 to 50.79 V rms.

Fig. 49 is a plot of THD versus SPL for ports, s, sr, a, b, and c, and Fig. 50 shows the same data for ports el, c, d, e, and f. At low sound pressure levels any flare works significantly better than a traditional straight port, and the more flare, the better. At medium SPL there is a clear trend that is revealed in the data for the ports examined in

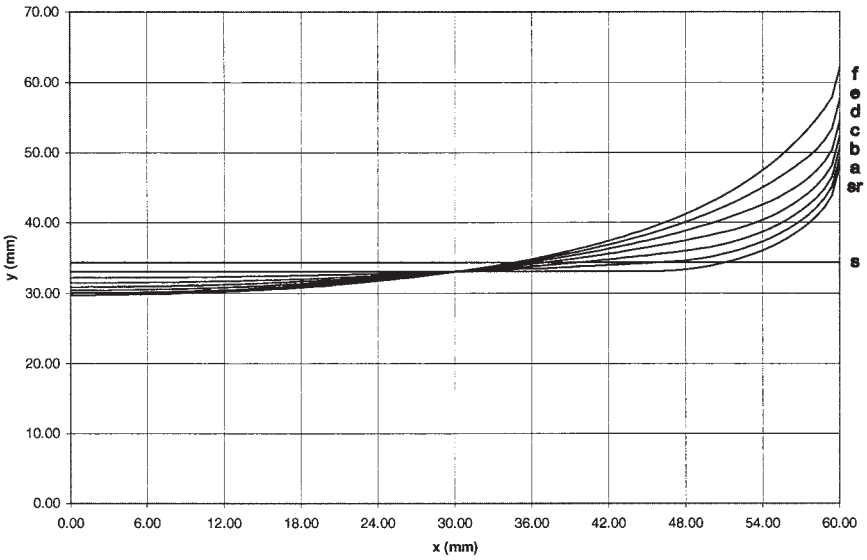

Fig. 48. Port profiles for polynomial study.

Table 1. Port characteristics.

Port Name	Physical Length (mm)	Minimum Diameter (mm)	Maximum Diameter (mm)	Max/Min Diameter	Max/Min Area	Tuning in 59-L Test Box (Hz)
s	120	68.7	68.7	1.00	1.00	33.0
sr	120	66.1	66.1	1.00	1.00	32.9
a	120	64.4	72.3	1.12	1.26	33.0
b	120	62.9	79.2	1.26	1.59	33.1
c	120	61.8	87.4	1.41	2.00	33.2
d	120	60.9	96.7	1.59	2.52	33.4
e	120	60.1	107.0	1.78	3.17	33.5
f	120	59.5	119.0	2.00	4.00	33.6
el	120	58.0	120.0	2.07	4.28	33.4

Fig. 49. Here performance is strongly related to the flare rate; the ports with more flare have lower distortion. For the ports with significant flare (Fig. 50) the differences are more subtle. At high SPL the performance gap becomes even tighter with no clear winners, only losers, that is, here the straight port actually outperforms ports sr and a. At high levels, however, ports c and d with a best fit NFR near 0.5 appear to have an edge.

These data lead us to the same conclusions found in Section 3.5, namely, that a generous flare, to a point, enhances port performance. There is some indication that too much flare is not necessarily a good thing. At medium SPL ports c and d perform nearly as well as the ports with more generous flares, and they appear to have an edge at higher levels. These differences, however, are extremely subtle when one compares the performance to ports sr, s, and a. Like the experiment with simple radii, the flare rates that are in the middle range are the best, and an optimum solution was achievable. The ellipse also performed quite well, suggesting that a different approach could be used to find a near optimum solution. The suggestion here is that there are probably an infinite number of profiles (all moderate in nature) that will perform well.

3.9 Port Asymmetry

In the previous experiment we noted that at high SPL ports c and d had the lowest odd harmonic distortion. In contrast, at high SPL ports c and d had a more even harmonic distortion than the others.

From our experience with transducers and amplifiers we tend to associate even harmonic distortion with asymmetry and odd harmonic distortion with symmetrical

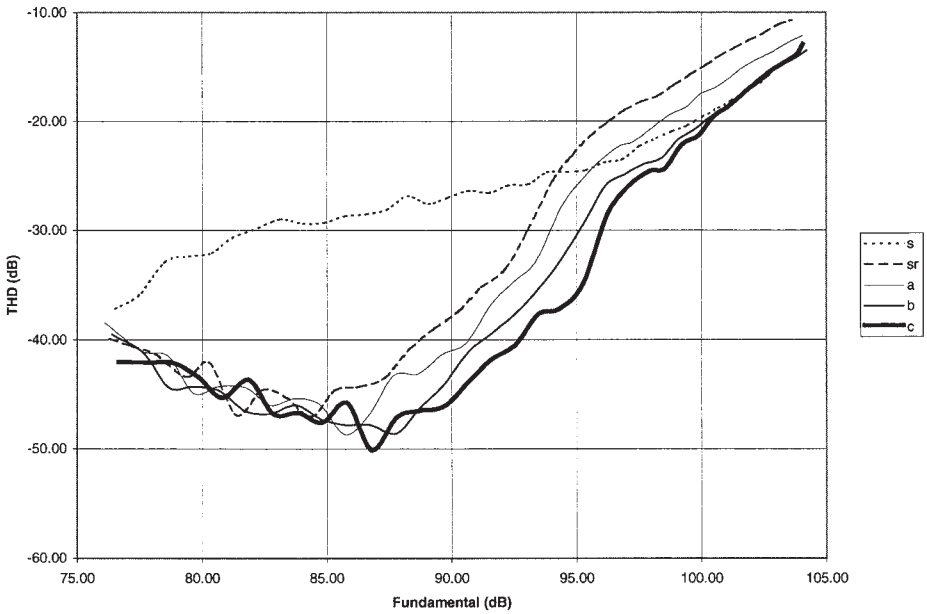

Fig. 49. THD versus fundamental for ports s (straight), sr (straight with radius), a, b, and c.

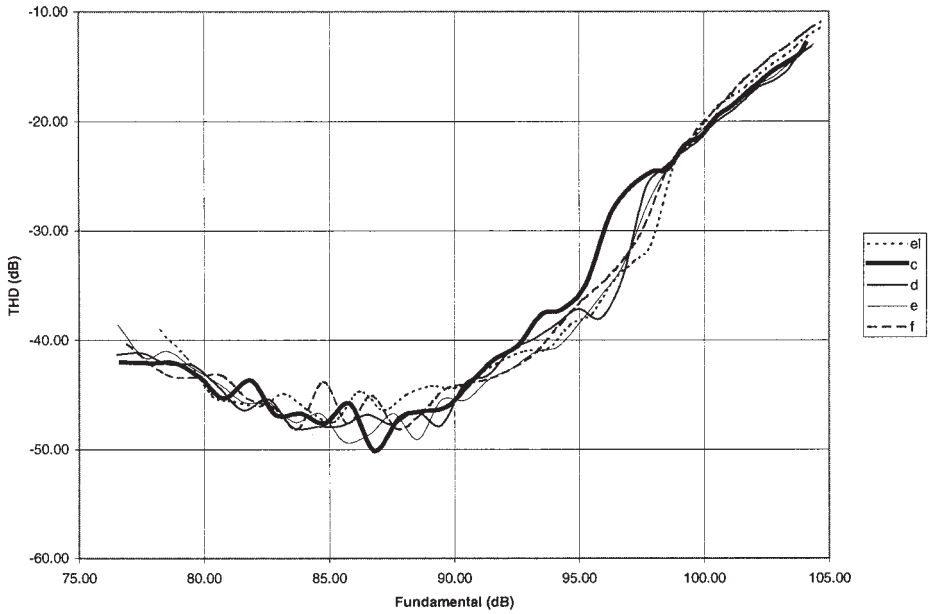

Fig. 50. THD versus fundamental for ports el (elliptical), c, d, e, and f.

"clipping." Could ports c and d have hidden asymmetry? All the ports were surface mounted in the enclosure. This means that one end of the port has a baffle and the other end does not. Thus all the ports were asymmetric. This suggests a preferential airflow in one direction over another, analogous to a fluid flow diode effect, and it can be thought of as "port rectification." Interestingly, the ports with the most generous flares, ports f and el, still have low even harmonic distortion at high SPL. It appears that the maximum diameter of these ports is enough to simulate a mounting baffle on the inside edge of the port. If this is true, then adding a simple flange to the inside of ports c and d should reduce even harmonic distortion. Fig. 51 shows even harmonic distortion for ports c and d and for the same ports with a small 15-mm-wide flange added to the inside (cf and df). A dramatic improvement is clearly seen in the even-order harmonic distortion, approaching 12 dB at the highest levels. It is clear that when choosing a port flare of moderate rate an additional design feature that should be incorporated is a flange on the inside of the port.

3.10 Thermal Implication of Port Design and Placement

In matters of the acoustical performance of a port, turbulence is the enemy. However, in matters of heat exchange, turbulence is a friend. If the acoustic port mass acts as a slug of air during laminar flow, it could be argued that the same slug of air moves in and out of the box and that no effective exchange of air from inside to outside occurs. The inside of a loudspeaker enclosure heats up as the components radiate heat into the box. In fact, it is not unusual for the air temperature in high-power designs to reach 200° F inside the enclosure. Temperatures this high limit the life of all components significantly, and it would therefore be desirable to keep the box as close to room temperature as possible. The ports in a vented box provide an ideal path for replacing the hot air in the box with cool ambient air, but if we have designed the port such that there is no net exchange, then the box will heat up and heat dissipation must occur through the walls. Turbulent air is extremely effective at dissipating heat as it rapidly mixes cool and warm air.

This line of thinking led the authors to speculate that smaller straight turbulent ports would have an advantage over well-designed larger tapered ports. To prove this hypothesis, an experiment was devised to test the heat dissipation of several port configurations. Fig. 52 shows the six configurations tested. Besides trying flared versus straight ports, we made the straight ports substantially smaller. We designed all ports to tune to about 25 Hz in a 12-ft^3 (0.34-m^3) box with a single 18-in (457-mm) driver. Experiments were run with one port and two ports. The condition with two ports placed one near the top and one near the bottom of the box, the idea being that with two ports in this configuration a convective "chimney effect" might provide additional cooling as cool air would come in at the bottom and warm air would exit the top. To take further advantage of this idea, a configuration was devised that had asymmetrical ports at the top and bottom, with the bottom port oriented to cause preferential airflow in the inward direction and the upper port oriented to provide preferential flow in the outward direction.

The measurement setup is also pictured in Fig. 52. A pink-noise signal of 20–2000 Hz was presented to the woofer. A broad-band signal was used so that a large amount of heat would be generated, but the port velocity in the case of the tapered ports would be low enough that they remain laminar, as only a small portion of the signal has energy near port tuning. The size of the smaller ports was chosen to ensure that they were in fact turbulent. The diameter of the tapered port was about 3.5 in (89 mm) and the smaller ports were about 1.75 in (44 mm). The tapered ports were also much longer (to ensure the same tuning). The amount of power to the system was monitored with a special device that also tracks voice-coil temperatures. A

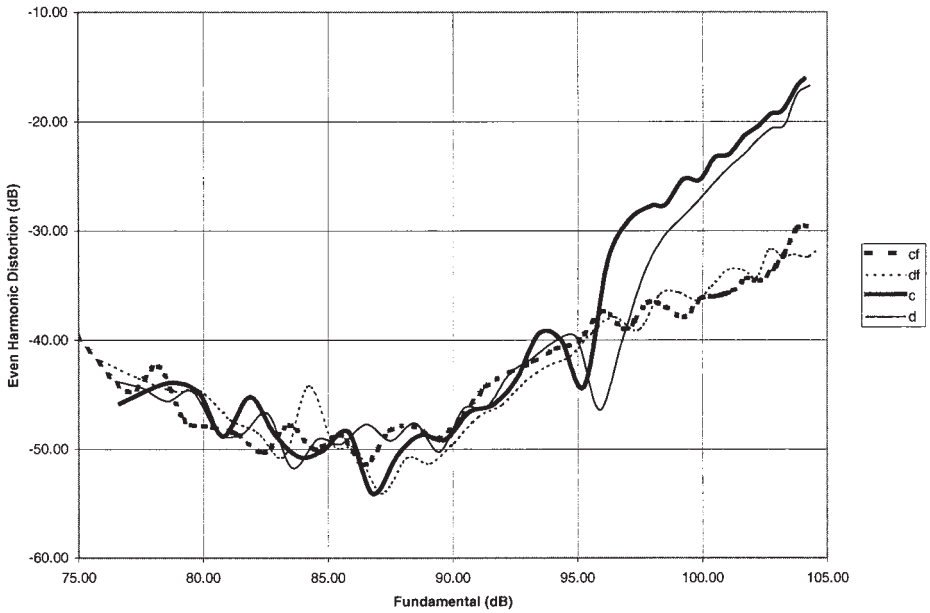

Fig. 51. Even harmonic distortion versus fundamental for ports cf (c with inside flange), df (d with inside flange), c, and d.

level of 250 W (true electrical power based on voltage and current, not dc resistance) was placed on the driver, and the voice-coil temperature and the in-box air temperature were monitored versus time.

Fig. 53 shows the results of all six trials. One trial was done with the box completely sealed. The air temperature results clearly show that all ported conditions cool the box significantly over the sealed box. The rise in the voice-coil temperature tracks the rise in the box temperature, except in the sealed box condition (which appeared not to have reached equilibrium and was still heating up after 3 hours). This would be expected. Interestingly the conditions that cooled the box the most were the two iterations with the small turbulent ports. The trial with two small ports outperformed all other configurations tested. Clearly, the turbulent flow and the arrangement of the ports at the top and bottom both contributed to an excellent heat exchange in the box. Is this tradeoff of lower temperature versus reduced port output worthwhile? Most likely not. The gains in maximum output of the system obtained by using well-designed ports should outweigh any thermal compression benefits gained through lowered box temperatures.

While the tapered ports performed poorly, it is a little surprising that the two asymmetrical tapered ports did not improve things as much as expected. Clearly the amount of dc flow due to the asymmetry was not substantial enough to create a significant heat exchange through the box. Turbulence exchanges heat far more effectively from the inside to the outside of the box than even large laminar ports. There may be a happy medium in running two asymmetrical ports slightly into turbulence, which would find a balance of compression, distortion, and heat dissipation.

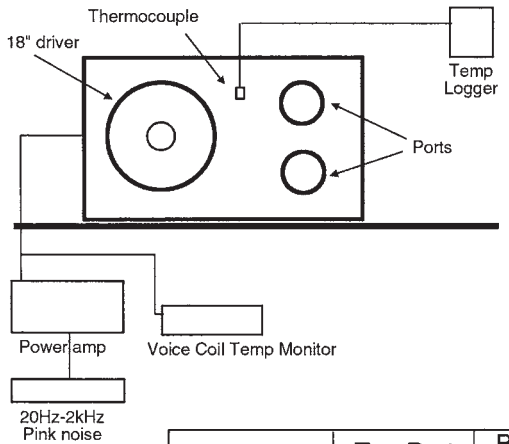

Trial	Top Port	Bottom Port
Sealed	X	X
2 double flared		
1 double flared		X
2 small holes		
1 small hole		X
innie/outie		

Fig. 52. Setup for thermal experiments.

4 GENERAL CONCLUSIONS

Based on the studies discussed, the following design rules should be applied to the design of loudspeaker ports:

1) Vast historical data and the results presented in this paper suggest that the largest port area allowable by a given design should be employed to keep the air velocity down if low port compression and low distortion are desired.

2) When designing a port for maximum acoustical output, both the inlet and the exit fluid dynamics should be balanced. The geometry for best exit flow is different from that for inlet flow. Inlet flow is best with a very large taper (NFR close to 1.0). For exit flow a very slow taper is best (NFR closer to 0). This points to an NFR of 0.5 as the optimum.

3) Inlet head loss should be minimized. Use port profiles that do not have any sharp discontinuities. This requires all port edges to have a blend radius of at least 20% of the minimum diameter.

4) For flared ports, choose an NFR to match the design application and intent. For lowest harmonic distortion at low levels, use NFRs near 1.0. At moderate levels, NFRs near 0.5 work best. At high levels, NFRs near 0 are desirable (though the blend radius in rule 3 should still be used). For the best compromise at all levels, NFR = 0.5

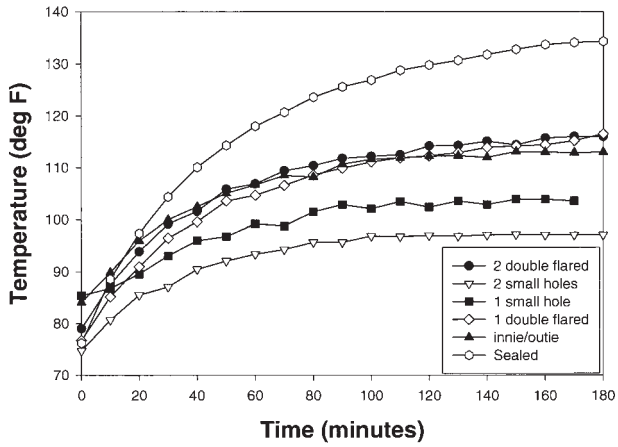

(a)

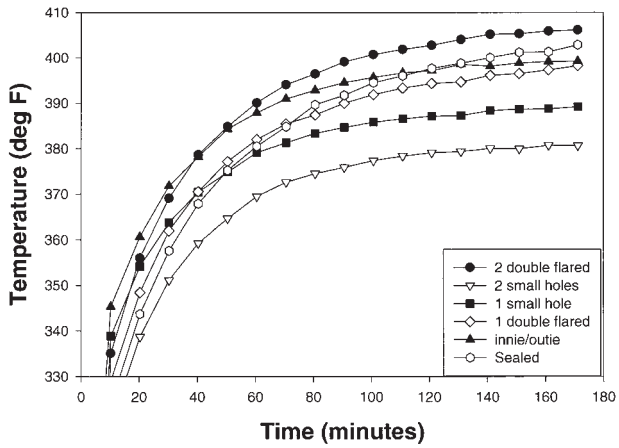

(b)

Fig. 53. Thermal repercussions for various port configurations versus time. (a) Box air temperature. (b) Voice-coil temperature.

appears to be optimum.

5) For best distortion performance at higher levels, make sure both sides of the port are symmetrical. Adding a small flange to the inside of a flush-mounted port makes a dramatic improvement in distortion.

6) Roughening the port walls generally does not appear to be beneficial in the normal operating range of acoustic ports.

7) In designing a flared port, the closer the radius used for the flare is to a simple radius, the simpler and more accurate the end correction can be, and the port tuning will be easy to calculate.

8) Maximally radiused ports have the best low-level performance, but they have poor high-level performance due to excessive turbulence within the port, near the ends. This will lead to compression and tuning shift due to the shortening of the apparent length of the port.

9) Large ports with a taper designed to minimize turbulence will act poorly to exchange the air (and heat) in the box. Ports that are in fact overdriven under maximum use and located at the top and bottom of the box would be preferred thermally.

10) There are many approaches to finding a port profile that will provide excellent performance. It is mainly the macroscopic shape and not the specific profile that influences performance.

5 ACKNOWLEDGMENT

The authors wish to thank Harman International, Mark Gander, and John Vanderkooy.

6 REFERENCES

[1] H. D. Harwood, "Loudspeaker Distortion Associated with Low-Frequency Signals," *J. Audio Eng. Soc.*, vol. 20, pp. 718–728 (1972 Nov.).

[2] R. Laupman, "Speaker System," U.S. patent 4,213,515 (filed 1978 Sept. 12; awarded 1980 July 22).

[3] J. Vanderkooy, "Loudspeaker Ports," presented at the 103rd Convention of the Audio Engineering Society, *J. Audio Eng. Soc. (Abstracts)*, vol. 45, p. 1006 (1997 Nov.), preprint 4523.

[4] J. Vanderkooy, "Nonlinearities in Loudspeaker Ports," presented at the 104th Convention of the Audio Engineering Society, *J. Audio Eng. Soc. (Abstracts)*, vol. 46, p. 576 (1998 June), preprint 4748.

[5] J. Backman, "The Nonlinear Behaviour of Reflex Ports," presented at the 98th Convention of the Audio Engineering Society, *J. Audio Eng. Soc. (Abstracts)*, vol. 43, p. 400 (1995 May), preprint 3999.

[6] N. B. Roozen, J. E. M. Vael, and J. A. M. Nieuwendijk, "Reduction of Bass-Reflex Port Nonlinearities by Optimizing the Port Geometry," presented at the 104th Convention of the Audio Engineering Society, *J. Audio Eng. Soc. (Abstracts)*, vol. 46, p. 576 (1998 June), preprint 4661.

[7] U. Ingard and H. Ising, "Acoustic Nonlinearity of an Orifice," *J. Acoust. Soc. Am.*, vol. 42, pp. 6–17 (1967).

[8] J. Young, "An Investigation into the Properties of Tubular Vents, as Used in a Helmholtz Resonator as Part of a Vented Box Loudspeaker System," Senior Thesis, University of Sydney, Australia, School of Mechanical Engineering (1975 Dec.).

[9] B. Gawronski and G. Caron, "Porting," U.S. patent 5,714,721 (awarded 1998 Feb. 3).

[10] M. Polk and C. Campbell, "Ported Loudspeaker System and Method with Reduced Air Turbulence," U.S. patent 5,517,573 (awarded 1996 May 14).

[11] M. Goto, "Acoustic Apparatus," U.S. patent 4,987,601 (awarded 1991 Jan. 22).

[12] S. Gahm, "Modular Port Tuning Kit," U.S. patent 5,623,132 (awarded 1997 Apr. 22).

[13] J. A. Pedersen and J. Vanderkooy, "Near-Field Acoustic Measurements at High Amplitudes," presented at the 104th Convention of the Audio Engineering Society, *J. Audio Eng. Soc. (Abstracts)*, vol. 46, p. 586 (1998 June), preprint 4683.

[14] M. C. A. M. Peters, A. Hirschberg, A. J. Reijnen, and A. P. J. Wijnands, "Damping and Reflection Coefficient Measurements for an Open Pipe at Low Mach and Low Helmholtz Numbers," *J. Fluid Mech.*, vol. 256, pp. 499–534 (1993).

[15] P. Merkli and H. Thomann, "Transition to Turbulence in Oscillating Pipe Flow," *J. Fluid Mech.*, vol. 68, pp. 567–575 (1975).

[16] M. R. Gander, "Dynamic Nonlinearity and Power Compression in Moving-Coil Loudspeakers," *J. Audio Eng. Soc.*, vol. 34, pp. 627–646 (1986 Sept.).

[17] C. Strahm, *Loudspeaker Enclosure Analysis Program*, Manual (1992).

[18] F. M. White, *Fluid Mechanics*, 3rd ed. (McGraw Hill, NY, 1994).

[19] L. L. Beranek, *Acoustics* (American Institute of Physics, New York, 1993).

7 BIBLIOGRAPHY

[20] L. Campos and F. Lau, "On Sound in an Inverse Sinusoidal Nozzle with Low Mach Number Mean Flow," *J. Acoust. Soc. Am.*, vol. 100(1) (1996 July).

[21] K. Furukawa, "Acoustic Apparatus," U.S. patent 5,109,422 (awarded 1992 Apr. 28).

[22] D. Y. Cheng, "Laminar Flow Elbow System and Method," U.S. patent 5,197,509 (awarded 1993 Mar. 30).

[23] T. Maxworthy, "Some Experimental Studies of Vortex Rings," *J. Fluid Mech.*, vol. 81 (1977).

[24] B. Seymour, "Nonlinear Resonant Oscillations in Open Tubes," *J. Fluid Mech.*, vol. 60 (1973).

[25] A. Cummings and W. Eversman, "High Amplitude Acoustic Transmission through Duct Terminations: Theory," *J. Sound Vibr.*, vol. 91 (1983).

[26] P. O. A. L. Davies, "Practical Flow Duct Acoustics," *J. Sound Vibr.*, vol. 124 (1988).

[27] L. Van Wijngaarden, "On the Oscillations Near and at Resonance in Open Pipes," *J. Eng. Math.*, vol. 2, no. 3 (1968).

[28] W. Chester, "Resonant Oscillations in Closed Tubes," *J. Fluid Mech.*, vol. 18 (1963).

[29] M. S. Howe, "The Interaction of Sound with Low

Mach Number Wall Turbulence, with Application to Sound Propagation in Turbulent Pipe Flow," *J. Fluid Mech.*, vol. 94 (1979).

[30] S. W. Rienstra, "Small Strouhal Number Analysis for Acoustic Wave–Jet Flow–Pipe Interaction," *J. Sound Vibr.*, vol. 86 (1983).

[31] M. C. A. M. Peters and A. Hirschberg, "Acoustically Induced Periodic Vortex Shedding at Sharp Edged Open Channel Ends: Simple Vortex Models," *J. Sound Vibr.*, vol. 161 (1993).

[32] J. H. M. Disselhorst and L. Van Wijngaarden, "Flow in the Exit of Open Pipes during Acoustic Resonance," *J. Fluid Mech.*, vol. 99 (1980).

[33] H. Levine and J. Schwinger, "On the Radiation of Sound from an Unflanged Circular Pipe," *Phys. Rev.*, vol. 73, no. 4 (1948).

THE AUTHORS

A. Salvatti

A. Devantier

D. Button

Alex Salvatti was born in 1973 and was raised in Southern California where he received an extensive musical education. He earned a B.S. degree in engineering physics with an acoustics specialization from the University of California at San Diego in 1996. After internships at IBM Storage Systems Division and TC Sounds, Inc, he joined JBL Professional as a transducer engineer where he has had design responsibilities for transducers including the LSR series of studio monitors and MPro line of sound reinforcement products. Mr. Salvatti is currently a senior research and development engineer with a professional focus on high-performance LF and HF transducer design. He has three patents in transducer design pending and is a member of the AES.

●

Allan Devantier was born 1964 June 6 in Newmarket, Ontario, Canada. He received a bachelor's degree in electrical engineering technology with honors in 1987 from Ryerson Polytechnical University in Toronto. He has been chief engineer for Infinity Systems, a division of Harman International located in Northbridge, California, since 1998 May. Prior to that, he spent three years as the director of systems engineering and three years as a systems engineer for JBL Consumer. He was systems engineer on Infinity's Prelude MTS loudspeaker system and is the inventor of Infinity's Room Adaptive Bass Optimization System and coinventor of the Ceramic Metal Matrix Diagram cone material (patent pending). Before joining Harman, he worked as a loudspeaker systems engineer for Plateau Camber and Belbois Ltee., both located in Montreal, Quebec. More recently, Mr. Devantier cochaired the loudspeaker student design competition that was held at the 140th meeting of the Acoustical Society of America. He is keenly interested in improving the correlation between the objective and subjective loudspeaker performance. He is married and has three children.

●

Douglas Button was born in 1959 in Fort Knox, Kentucky. He was educated at Iowa State University where he received a B.S.E.E. in 1982. He is currently vice president of research and development for JBL Professional in Northridge, California. He has been with JBL since 1988. Before that he worked for Harris Broadcast products from 1983 to 1985 and Electro-Voice from 1985 to 1987. He holds six patents with five pending. The focus of his work has been maximizing performance through innovative designs. JBL products of his invention include the high-power Vented Gap Cooling transducers, Neodymium Dual Coil Drivers and the EON Thermal Management System along with recent ultralight compression driver designs utilizing beryllium diaphragms.

Mr. Button has participated in several AES workshops on loudspeaker design and has delivered six papers on transducer design to AES conventions of which three have been published in the *Journal*. He has been a regular contributor to the AES Technical Committee on Transducers and previously served as a member of the executive committee of the AES Los Angeles Section. In 1997 Mr. Button was made a fellow of the AES.